



## Discovery and rational design of 2-aminopyrimidine-based derivatives targeting Janus kinase 2 (JAK2) and FMS-like tyrosine kinase 3 (FLT3)

Yingxiu Li, Peng Wang, Cong Chen, Tianyu Ye, Yufei Han, Yunlei Hou, Yajing Liu, Ping Gong, Mingze Qin\*, Yanfang Zhao\*

Key Laboratory of Structure-Based Drug Design and Discovery, Ministry of Education, Shenyang Pharmaceutical University, 103 Wenhua Road, Shenhe District, Shenyang 110016, China

### ARTICLE INFO

#### Keywords:

2-Aminopyrimidine derivatives  
Structure–activity relationships  
JAK2/FLT3 dual inhibitor

### ABSTRACT

Herein, with the help of computer-aided drug design (CADD), we describe the structure-based rational drug design, structure–activity relationships, and synthesis of a series of 2-aminopyrimidine derivatives that inhibit both JAK2 and FLT3 kinases. These screening cascades revealed that compound **14I** demonstrated the most inhibitory activity with IC<sub>50</sub> values of 1.8 and 0.68 nM against JAK2 and FLT3 respectively. **14I** also showed potent anti-proliferative activities against HEL (IC<sub>50</sub> = 0.84 μM) and Molm-13 (IC<sub>50</sub> = 0.019 μM) cell lines, but relatively weak cytotoxicity against K562 and PC-3 cell lines, which proved that it might have high target specificity. *In vitro* metabolism assay, **14I** exhibited moderate stability in RLM (Rat Liver Microsomes) with a half-life time of 31 min. In the cellular context of Molm-13, **14I** induced cell cycle arrest in G<sub>1</sub>/S phase and enhanced apoptosis in a dose-dependent manner. These results indicate that **14I** is a promising dual JAK2/FLT3 inhibitor and worthy of further development.

### 1. Introduction

Malignant hematological tumors are a group of malignant clonal diseases derived from the hematopoietic system, including myelodysplastic syndrome, myeloproliferative diseases, malignant lymphoma and leukemia. Among them, acute myeloid leukemia (AML), one of the most common types of adult acute leukemia, is a clinically and genetically heterogeneous disease with a poor prognosis in the majority of the patients [1]. At present, the combination of cytarabine (Ara-C) and an anthracycline (e.g., either idarubicin or daunorubicin) are still used as frontline induction chemotherapy for patients with AML, particularly those younger than 65 years of age [2]. However, those chemotherapeutic drugs have limited effects on AML as well as serious side effects. In contrast, small-molecule-targeted drugs show advantages of higher specificity and lower toxicity profile. Therefore, discovery of small-molecule-targeted drugs has become a promising strategy for treating acute myeloid leukemia.

FMS-like tyrosine kinase 3 (FLT3), also known as CD135 (Cluster of differentiation antigen 135) or Flk2 (fetal liver kinase-2), is a receptor tyrosine kinase compiled by FLT3 gene [3]. FLT3 plays a crucial role in the development of hematopoietic progenitor cells, and the abnormal

activation of FLT3 is closely related to the occurrence and development of various tumors, especially AML [4]. Besides, the FLT3 mutation is also one of the most common genetic mutations in AML patients, up to 45% of patients with AML have been shown to have FLT3 mutations [5]. There are two main types of activating mutations in FLT3: internal tandem duplication (ITD) mutations in the juxtamembrane domain and point mutations in the activation loop of the tyrosine kinase domain (TKD). Mutation of FLT3 can cause excessive activation of the FLT3 signalling pathway, leading to the disorder of hematopoietic system function, and plays an important role in the pathogenesis of AML. Developing FLT3 inhibitors have become one of the hottest research fields of anti-AML drugs.

At present, several FLT3 inhibitors have been launched or entered clinical trials (Fig. 1), such as midostaurin (PKC412, approved by FDA in April 2017) [6], gilteritinib (approved by FDA in November 2018) [7] and quizartinib (AC220, approved in Japan in June 2019) [8]. Although positive outcomes were obtained for these FLT3 inhibitors during clinical trials, most patients experienced rapid drug-resistant relapse, which has become a major challenge in treating AML [9,10]. Studies have shown that designing dual-inhibitors based on FLT3 is one of the most effective ways to overcome this resistance [11], and many dual-

\* Corresponding authors.

E-mail addresses: [qinmingze001@126.com](mailto:qinmingze001@126.com) (M. Qin), [yanfangzhao@126.com](mailto:yanfangzhao@126.com) (Y. Zhao).

<https://doi.org/10.1016/j.bioorg.2020.104361>

Received 12 August 2020; Received in revised form 5 October 2020; Accepted 6 October 2020

Available online 9 October 2020

0045-2068/© 2020 Elsevier Inc. All rights reserved.

inhibitors have been reported, such as gilteritinib (FLT3/Axl) [12], AMG 925 (FLT3/CDK4) [13], pacritinib (FLT3/JAK2) [14].

Janus kinase 2 (JAK2) is an intracellular non-receptor tyrosine kinase that belongs to the JAK kinase family (JAK1, JAK2, JAK3 and TYK2). JAK2-STAT5 is one of the downstream pathways of FLT3 and plays a vital role in the production of bone marrow, red blood cells and platelets. The excessive activation of the JAK2-STAT5 pathway leads to the cause of malignant hematological tumors [15,16].

The mutual promotion of JAK2 and FLT3 was observed in patients with AML. High level of FLT3 is accompanied by a significant increase in phosphorylated JAK2 (p-JAK2) level in AML patients. Also, in AML patients with FLT3-ITD mutation, the content of negative regulators of JAK2 is concomitantly reduced, resulting in the elevation of phosphorylated STAT5 (p-STAT5), which leads to abnormal proliferation of AML cells [17]. These discoveries indicate that simultaneously inhibiting FLT3 and JAK2 can synergistically down-regulate the p-STAT5 level, thereby more effectively delay the progression of AML. As a result, JAK2/FLT3 dual inhibitors were expected to overcome the development of drug resistance and improve treatment outcomes in AML patients. Fedratinib (**1**), the only launched JAK2/FLT3 dual inhibitor, was approved by FDA in August 2019 for the treatment of myelofibrosis [18]. Pacritinib (SB1518, **2**) is another reported JAK2/FLT3 dual inhibitor which is under Phase III for the treatment of myelofibrosis, and its clinical trial for AML is in Phase II now [19].

Previously, we reported the discovery of a series of novel JAK2/FLT3 dual inhibitors with 4-piperazinyl-2-aminopyrimidine as scaffold [20]. It has been identified that compound **3** inhibits JAK2 and FLT3 with  $IC_{50}$  values of 27 nM and 30 nM, respectively. In this paper, based on previous work and guided by computer-aided drug design (CADD), the lead compound **3** was modified in the pyrimidine ring and piperazine ring successively, then a series of 2-aminopyrimidine compounds were obtained. Designed compounds were screened for their JAK2/FLT3 enzymatic inhibitory and cellular anti-proliferative activities in a panel of leukemia cell lines. Using flow cytometry, the cell cycle and apoptosis effects of **14i** on Molm-13 were examined to elucidate the primary

mechanism. The stability of potent compounds in rat liver microsomes were also evaluated.

## 2. Results and discussion

### 2.1. *In silico* analysis and design of compounds

Using Schrödinger Glide, the molecular docking analysis was performed with **3** to assess its binding with JAK2 and FLT3, respectively. As shown in Fig. 2, we found that the hydrophobic cavity of JAK2 which was composed of backbone ALA880, MET929, GLU930 and LEU993 was not completely occupied by 4-piperazinyl-2-aminopyrimidine scaffold, and the same situation can be found in the docking with FLT3 (related residues are ALA648, GLU692, Leu746 and CYS756). In order to make the hydrophobic cavity fully occupied by the molecule, different groups (such as methyl, halogen, aromatic rings, etc.) were introduced to the 5- or 6- position of pyrimidine ring to afford compounds **14a-14o**.

On the other hand, the piperazinyl-aryl-urea fragment was observed to locate in the P-loop (phosphate-binding loop) region of JAK2 and FLT3. It is known that the P-loop is responsible for binding the ATP's phosphate chain, and the amino acid sequences of P-loop are glycine-rich [21]. Therefore, in the design of tyrosine kinase inhibitors (TKIs), the P-loop region is a hot spot for the construction of hydrogen bonding [22–24]. However, only one hydrogen bond was observed between the urea moiety and LYS650 of FLT3. In order to increase the hydrogen-bonding between molecule and P-loop, thus enhancing the kinase inhibitory activities, we modified the piperazinyl-aryl-urea fragment and obtained compounds **15a-15h** and **16a-16h**.

The design strategy was shown in Fig. 3. All designed compounds were evaluated for their JAK2/FLT3 enzymatic inhibitory activities, and the anti-proliferative effects on HEL and Molm-13 cell lines were also assayed.

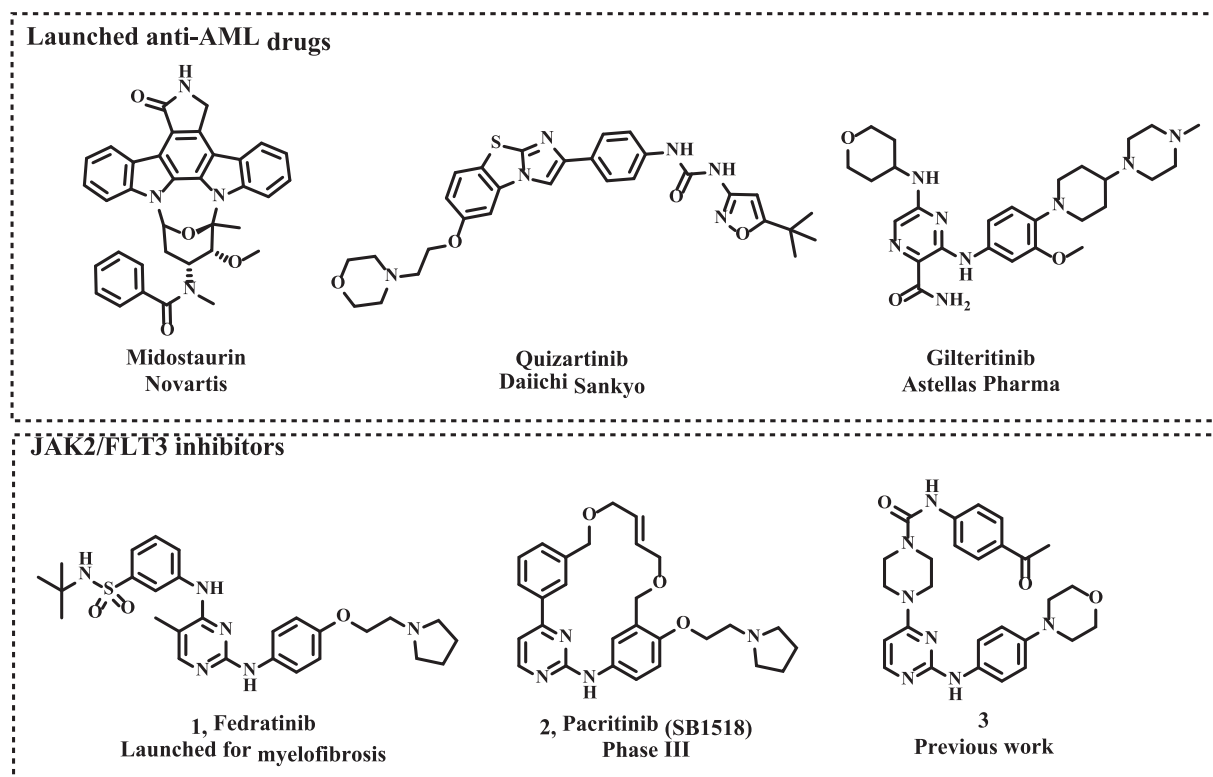
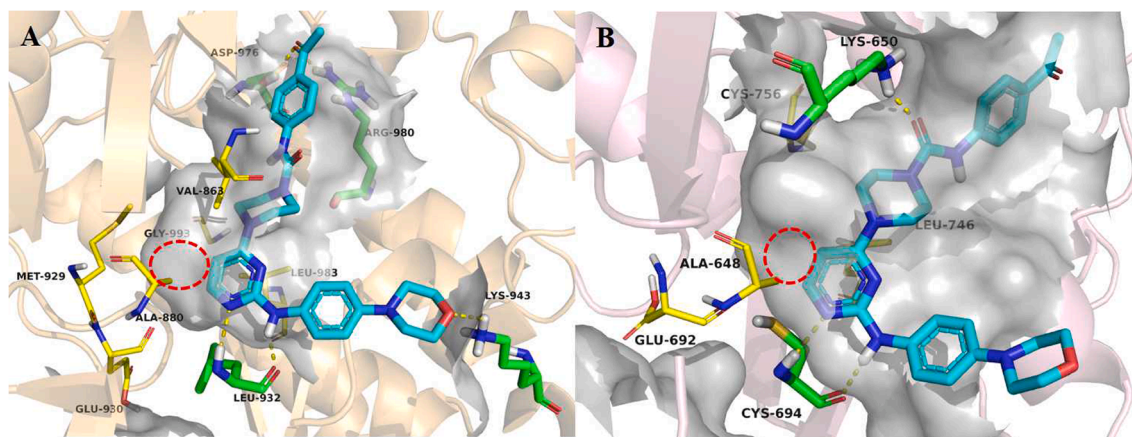
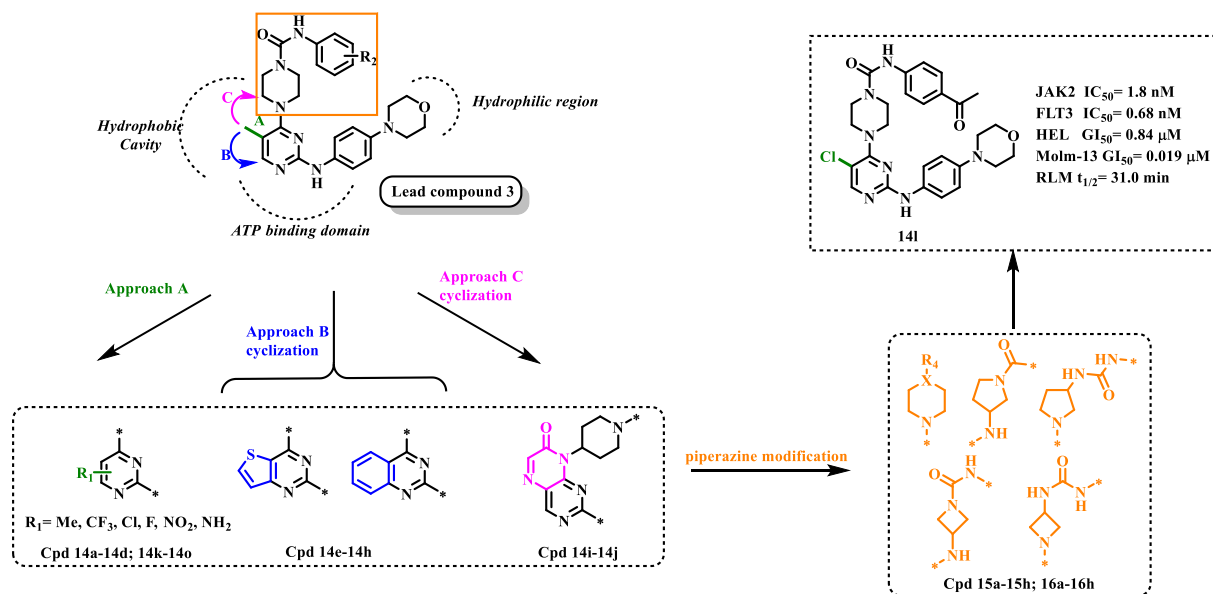


Fig. 1. The chemical structures of FLT3 or JAK2/FLT3 inhibitors that have been launched or reported.



**Fig. 2.** Proposed binding modes between compound **3** and JAK2 and FLT3 kinase; hydrogen bonds shown as yellow dashed lines; residues that composed the hydrophobic cavities were colored in yellow; the hydrophobic cavities were marked by red circle. (A) Compound **3** was docked into the ATP-binding site of JAK2 (PDB code 4JI9). (B) Compound **3** was docked into the ATP-binding site of FLT3 (homology modelling). (For interpretation of the references to colour in this figure legend, the reader is referred to the web version of this article.)



**Fig. 3.** The design strategy based on the molecular docking.

## 2.2. Chemistry

As shown in Scheme 1, the synthetic route was described. Target compounds **14a-h**, **15a-h** and **14k-o** were synthesized from commercially available 2,4-dichloropyrimidine derivatives (**4a-h**) in four steps as described previously [20].

For pteridinone derivatives, 2,4-dichloro-5-nitropyrimidine (**4h**) reacted with 1-Boc-4-aminopiperidine to give **5i**, which was then condensed with 4-morpholinoaniline to give **6i**. **6i** was subsequently reduced to corresponding intermediate **7i** in the presence of H<sub>2</sub>-Pd/C. After the treatment of **7i** with 50% ethyl glyoxylate in toluene and deprotection of *N*-Boc group, intermediate **9** was obtained [25]. Then, **9** was reacted with Phenyl *N*-(4-acetylphenyl)carbamate (**10**) or acetyl acid to afford **14i-j**, respectively.

Intermediates **6j-m** were synthesized according to the above route. **6j** was hydrolyzed in the presence of sodium hydroxide and then reacted with 4-aminoacetophenone and 4-acetylbenzoxonitrile to give **16a-b**, respectively. Intermediates **6k-m** reacted with phenyl *N*-(4-acetylphenyl)carbamate (**10**) or acetyl acid to yield **7k-m**. Subsequently, target compounds **16c-f** were obtained through the substitution of **7k-m**

with 4-morpholinoaniline under the catalysis of trifluoroacetic acid in sealed-tubes.

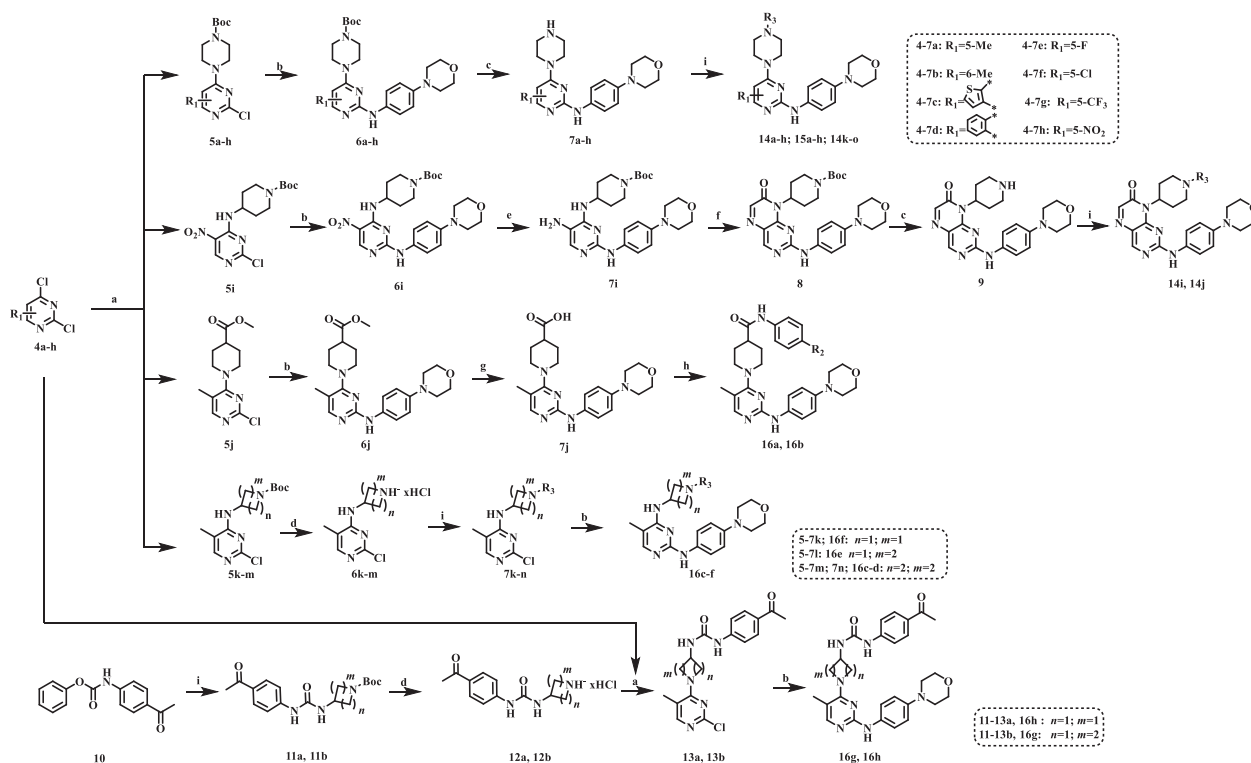
For compounds **16g-h**, intermediates **12a-b** were firstly synthesized and then reacted with 5-methyl-2,4-dichloropyrimidine (**4a**) to yield intermediates **13a-b**. Finally, **13a-b** reacted with 4-morpholinoaniline to afford **16g-h**.

## 2.3. Biological evaluation

### 2.3.1. In vitro kinase and cellular biological activities

Compounds **14a-j** were firstly synthesized, the results of the kinase-inhibition and cell anti-proliferation assays were listed in Table 1 with compound **3** as the positive control.

As shown in Table 1, compounds with a methyl group at 5-position of pyrimidine ring showed more enhanced JAK2 and FLT3 inhibitory activities than those at 6-position (**14a-d**), and compounds (**14e-j**) with sterically large groups such as binary heteroaromatic rings showed less potency. Along with the decline in kinase activities, compounds **14c-j** showed weaker cellular potency against HEL (JAK2-dependent) and Molm-13 cell lines (FLT3-dependent) than **14a** and **14b**.



**Scheme 1.** Synthetic route for designed compounds; **Reagents and conditions:** (a) Et<sub>3</sub>N, DMF, rt, 4 h; (b) 4-morpholinoaniline, TFA, *i*-PrOH, 100 °C, sealed-tubes; (c) TFA, DCM, rt, 12 h; (d) 4 M HCl/EA, rt, 12 h; (e) Pd-C, H<sub>2</sub>, EtOH, 12 h; (f) EtOOC – CHO, HOAc, EtOH, reflux, 5 h; (g) 1 M NaOH, MeOH, 60 °C, 2 h; (h) HATU, DIPEA, 1,4-dioxane, 0 °C to rt, 12 h; (i) (1) phenyl carbamates, DIPEA, DMF, 40 °C, 12 h; (2) acid chlorides, TEA, DCM, –10 °C to 0 °C.

Docking **14a** into the JAK2 and FLT3 ATP-binding sites supported the hypothesis that the expected binding mode is preferred with a substituent at 5-position of pyrimidine ring. As shown in Fig. 4, the methyl group at 5-position of pyrimidine fits well into the hydrophobic cavity of JAK2 (bound by the backbone ALA880, MET929, GLU930 and LEU993) and FLT3 (bound by the backbone ALA648, GLU692 and LEU746). In contrast, due to steric restrictions, the methyl group in 6-position of pyrimidine ring may conflict with those backbone residues, resulting in reduced JAK2 and FLT3 activities. The steric restrictions may also cause the decrease in activities of binary aromatic heterocycles derivatives.

Considering that **14a** and **14b** showed better potency than lead compound **3**, we selected **14a** and **14b** for further optimization (Table 2). At this stage, the piperazinyl-aryl-urea fragment was modified to obtain a series of carbonyl and sulfonyl derivatives (see **15a-h**). As compared with **14a**, the anti-proliferative effects of compounds **15a-h** on HEL and Molm-13 cell lines were significantly reduced, although some of them (**15d**, **15g**, and **15h**) still retained moderate inhibitory activities against JAK2 and FLT3. So we believed that the existence of aromatic rings was necessary, then designed amide analogues **16a-b**. Their kinase activities were comparable to that of **14a**, but their cellular anti-proliferative effects were not remarkable as compared with **14a**.

Next, we turned our attention to the piperazinyl ring. Compounds **16c** and **16d** containing a 4-aminopiperidinyl moiety instead of piperazine exhibited comparable kinase inhibitory activities with **14a** (4-aminopiperazinyl moiety) but displayed weaker anti-proliferative activities against cancer cells than **14a**. Then, the size of aliphatic ring was reduced and compounds **16e-h** were obtained. 3-aminopyrrolidinyl derivatives (**16e**, **16g**) showed moderate inhibitory activity against JAK2 and FLT3, and 3-aminoazetidyl derivatives (**16f**, **16h**) exhibited weak activities against two kinases at 100 nM. Clearly, the piperazinyl moiety fills out the available space in the binding site better than other aliphatic rings. Taken together, optimizing the piperazinyl-aryl-urea fragment did not significantly improve the efficiencies of the compounds.

As compared with **3**, compound **14a** with a methyl group at 5-position of pyrimidine ring exhibited 9-fold and 21-fold higher potency against JAK2 and FLT3, respectively (see Table 1). In order to further investigate the effects of substituents at 5-position of pyrimidine, compounds **14k-o** were synthesized (Table 3). Surprisingly, 5-halogen substituted analogues exhibited both more potent kinase activities and anti-proliferative activities than **14a**, while a slight decrease of kinase and cellular potency occurred in compounds **14m-o**.

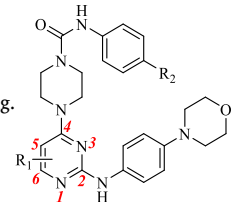
Given that compounds **14a**, **14k**, and **14l** exhibited desirable *in vitro* kinase and cellular activities, they were shortlisted for further biochemical profiling with fedratinib (**1**) and pacritinib (**2**) as positive control (Table 4). Two JAK2/FLT3-independent tumor cell lines were also employed in this assay (K562, PC-3). The tested compounds all exhibited potent inhibitory activities against JAK2 and FLT3 kinases, and also exerted potent anti-proliferative activities against HEL (in the range of 0.5–0.8 μM) and Molm-13 cell lines (in the range of 0.019–0.042 μM), while significantly less sensitiveness to K562 and PC-3 were observed. Among them, 5-chloro-substituted compounds **14l** showed the most potent inhibitory activities against JAK2 (IC<sub>50</sub> = 1.8 nM) and FLT3 (IC<sub>50</sub> = 0.68 nM) kinases. Comparing with Fedratinib, **14l** had superior inhibitory activities against FLT3, HEL cells and Molm-13 cells. For non-JAK2/FLT3 dependent cells (PC-3 and K562), **14l** showed better selectivity than Fedratinib (**1**) and Pacritinib (**2**), indicating a better safety profile.

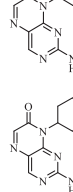
### 2.3.2. Assessment of *in vitro* metabolism

Liver microsomal stabilities indicated significant phase 1 metabolism events. The preliminary metabolic-stability study of compounds **3**, **14a**, **14k** and **14l** were performed by using rat liver microsomes (RLM, Table 5). Compound **3** had a half-life of 120.2 min and intrinsic liver clearance of 20.7 μL/min/mg, which indicated that compound **3** was quite stable in RLM. Even though, 5-substituted pyrimidine derivatives **14a**, **14k** and **14l** were cleared more rapidly than **3**, they were still comparable with Pacritinib (**2**) which was reported to have a half-life in

Table 1

SAR exploration of substituents on the pyrimidine ring.



Compd	R <sub>1</sub>	R <sub>2</sub>	JAK2 inhibition @ 100 nM <sup>a</sup>	FLT3 inhibition @ 100 nM <sup>a</sup>	HEL IC <sub>50</sub> ± SD (μM) <sup>b</sup>	Molm-13 IC <sub>50</sub> ± SD (μM) <sup>b</sup>
3	–	–COCH <sub>3</sub>	86.7% (27 nM) <sup>c</sup>	80.7% (30 nM) <sup>c</sup>	4.3 ± 0.6	0.077 ± 0.004
14a	5-Me	–COCH <sub>3</sub>	81.8% (2.9 nM) <sup>c</sup>	99.1% (1.4 nM) <sup>c</sup>	0.8 ± 0.2	0.042 ± 0.002
14b	5-Me	–CN	88.5%	95.2%	0.9 ± 0.2	0.072 ± 0.002
14c	6-Me	–COCH <sub>3</sub>	15.6%	20.9%	>10	>0.5
14d	6-Me	–CN	8.9%	15.8%	>10	>0.5
14e		–COCH <sub>3</sub>	44.0%	68.0%	3.5 ± 0.9	>0.5
14f		–CN	17.6%	69.4%	4.1 ± 0.5	>0.5
14g		–COCH <sub>3</sub>	3.2%	36.0%	3.0 ± 0.2	>0.5
14h		–CN	9.7%	40.5%	3.2 ± 0.4	>0.5
14i			2.3%	35.9%	5.8 ± 0.2	0.079 ± 0.003
14j			3.5%	16.7%	7.7 ± 0.3	>0.5

<sup>a</sup> The average is indicated (n ≥ 2 independent experiments).

<sup>b</sup> Data was reported as the average of at least three replicates, SD: standard deviation.

<sup>c</sup> The IC<sub>50</sub> values of Compounds 3 and 14a were averaged (n ≥ 2 independent experiments).

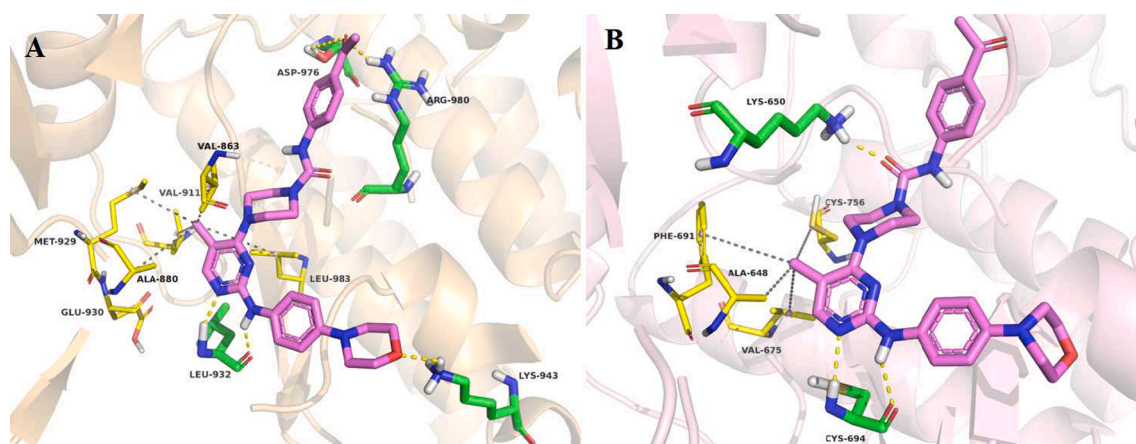


Fig. 4. Compound 14a docked into (A) JAK2 and (B) FLT3; hydrogen bonds were shown as yellow dashes; hydrophobic interactions were shown as grey dashes. (For interpretation of the references to colour in this figure legend, the reader is referred to the web version of this article.)

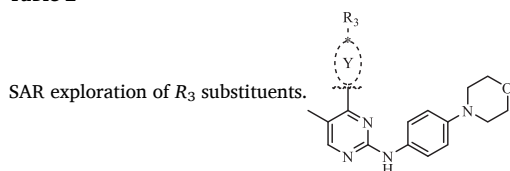
RLM of 18 min [14]. Considering that compound 14i showed optimal bioactivities and moderate stability in RLM, we selected 14i as a candidate for further studies.

### 2.3.3. Kinase selectivity profiling of 14i

Given the fact that 14i exhibited the desirable in vitro biochemical

activities as well as moderate stability in RLM, 14i was further chosen to examine its kinase selectivity profile containing 20 kinases (scanEDGE KINOMEScan, DiscoverX) at a compound concentration of 30 nM. As shown in Fig. 5., 14i did not show sufficient activities to this panel of kinases except for the JAKs and FLT3s, illustrating certain kinase selectivity for this pyrimidine chemotype. However, 14i did not show

Table 2



Compd	Y	$R_3$	JAK2 inhibition @ 100 nM <sup>a</sup>	FLT3 inhibition @ 100 nM <sup>a</sup>	HEL IC <sub>50</sub> ± SD (μM) <sup>b</sup>	Molm-13 IC <sub>50</sub> ± SD (μM) <sup>b</sup>
14a			81.8%	99.1%	0.8 ± 0.2	0.042 ± 0.002
15a			66.2%	45.3%	>10	>0.5
15b			1.0%	16.7%	>10	>0.5
15c			73.4%	41.7%	>10	0.31 ± 0.03
15d			63.4%	68.0%	>10	>0.5
15e			56.4%	9.5%	>10	>0.5
15f			77.0%	31.4%	>10	>0.5
15g			76.2%	51.7%	>10	>0.5
15h			82.4%	54.5%	>10	>0.5
16a			74.3%	97.0%	1.7 ± 0.2	0.062 ± 0.06
16b			72.8%	94.3%	1.3 ± 0.4	0.035 ± 0.03
16c			70.5%	53.9%	>10	>0.5
16d			80.5%	78.6%	6.7 ± 0.7	0.35 ± 0.04
16e			69.3%	57.3%	>10	>0.5
16f			8.1%	16.2%	>10	>0.5
16g			57.4%	75.7%	>10	0.22 ± 0.03
16h			21.9%	50.0%	>10	>0.5

<sup>a</sup> The average is indicated ( $n \geq 2$  independent experiments).

<sup>b</sup> Data was reported as the average of at least three replicates, SD: standard deviation.

distinct selectivity among JAKs family (JAK1 = 76.36%, JAK2 = 80%, JAK3 = 50.91%), which is likely to result in some side effects and risks. Therefore, this is an urgent problem to be solved in subsequent works.

#### 2.3.4. Compound **14l** induced $G_1/S$ cell cycle arrest

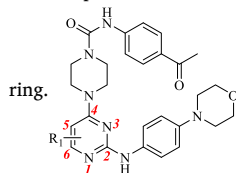
The cell cycle analysis of desirable compound **14l** on Molm-13 cells was assessed using flow cytometry and the results were shown in Fig. 6. Significant  $G_1/S$  transition arrest was observed in Molm-13 cells treated with **14l**. The percentage of cells in the  $G_1$  phase was remarkably increased from 43.12% (non-treated) to 90.27% (0.2 μM **14l**-treated) and the fraction of cells in  $G_1$  phase was dose-dependently increased.

#### 2.3.5. Compound **14l** induced apoptosis of Molm-13 cells

The apoptosis of Molm-13 cells was analysed after treated with different concentrations of the optimal derivative **14l**. As detected by annexin V staining, a dose-dependent increase in the percentage of apoptotic and dead cells was observed, which is consistent with the increased  $G_1/S$  cell population observed in Molm-13 cells (Fig. 7). In the presence of vehicle alone for 48 h, 3.8% of the cells were in apoptosis. Treatment with 0.2 μM compound **14l** for 48 h led to an increase in the degree of apoptosis by 64.6%. Hence, these results demonstrated that **14l** induced effective apoptotic effects in Molm-13 cells.

**Table 3**

SAR optimization of substituents at 5-position of pyrimidine



Compd	R <sub>1</sub>	JAK2 inhibitor @ 100 nM <sup>a</sup>	FLT3 inhibition @ 100 nM <sup>a</sup>	HEL IC <sub>50</sub> ± SD (μM) <sup>b</sup>	Molm-13 IC <sub>50</sub> ± SD (μM) <sup>b</sup>
14k	5-F	93.5%	99.3%	0.7 ± 0.2	0.026 ± 0.004
14l	5-Cl	99.4%	98.7%	0.5 ± 0.1	0.019 ± 0.001
14m	5-CF <sub>3</sub>	74.6%	82.5%	4.6 ± 0.6	0.083 ± 0.002
14n	5-NO <sub>2</sub>	68.4%	97.8%	7.7 ± 0.2	0.27 ± 0.04
14o	5-NH <sub>2</sub>	22.8%	67.9%	>10	>0.5

<sup>a</sup> The average is indicated (n ≥ 2 independent experiments).<sup>b</sup> Data was reported as the average of at least three replicates, SD: standard deviation.**Table 4***In vitro* biochemical profiling of 14l.

Compd	JAK2 IC <sub>50</sub> (nM) <sup>a</sup>	FLT3 IC <sub>50</sub> (nM) <sup>a</sup>	HEL IC <sub>50</sub> ± SD (μM) <sup>b</sup>	Molm-13 IC <sub>50</sub> ± SD (μM) <sup>b</sup>	K562 IC <sub>50</sub> ± SD (μM) <sup>b</sup>	PC-3 IC <sub>50</sub> ± SD (μM) <sup>b</sup>
1	1.5 <sup>c</sup>	24 <sup>c</sup>	0.9 ± 0.1	0.068 ± 0.003	0.56 ± 0.05	5.5 ± 0.3
2	10 <sup>d</sup>	1.8 <sup>d</sup>	1.1 ± 0.2	0.023 ± 0.001	0.68 ± 0.04	8.7 ± 0.4
14a	2.9	1.4	0.8 ± 0.2	0.042 ± 0.002	1.4 ± 0.1	>20
14k	7.3	1.3	0.7 ± 0.2	0.026 ± 0.004	3.5 ± 0.5	>20
14l	1.8	0.68	0.5 ± 0.1	0.019 ± 0.001	4.3 ± 0.2	>20

<sup>a</sup> The average is indicated (n ≥ 2 independent experiments).<sup>b</sup> Data was reported as the average of at least three replicates, SD: standard deviation.<sup>c</sup> Fedratinib's activity data in reference literature is JAK2 = 3 nM and FLT3 = 15 nM. *Cancer Cell* 13(4), 311–320.<sup>d</sup> Pacritinib's activity data in reference literature is JAK2 = 22 nM and FLT3 = 23 nM. *J. Med. Chem* 2011, 54, 4638–4658.

### 2.3.6. Molecular modeling simulations

As the optimal compound **14l** exhibited optimal kinase inhibitory activities against JAK2 and FLT3, and strong anti-proliferative activity in HEL and Molm-13 cell lines. Thus, to elucidate the potential binding

**Table 5***In vitro* parameters of Rat Liver Microsomes Stability.

Compd	R <sup>2</sup> <sup>a</sup>	T <sub>1/2</sub> (min)	CL <sub>int(mic)</sub> (μL/min/mg) <sup>b</sup>	CL <sub>int(liver)</sub> (μL/min/mg) <sup>c</sup>	Remaining (T = 60 min)	Remaining (NCF = 60 min) <sup>d</sup>
3	0.8906	120.2	11.5	20.7	69.1%	83.5%
14a	0.8933	41.9	33.1	59.6	34.9%	96.2%
14k	0.9171	48.8	28.4	51.1	40.2%	93.9%
14l	0.9791	31.0	44.7	80.5	26.5%	90.7%
Propafenone	0.9705	1.3	1047.3	1885.1	0.4%	98.0%
Diclofenac	0.9907	23.4	59.3	106.7	16.9%	96.3%

<sup>a</sup> R<sup>2</sup>: coefficient of determination.<sup>b</sup> CL<sub>int(mic)</sub>: intrinsic clearance; CL<sub>int(mic)</sub> = 0.693/T<sub>1/2</sub>/mg microsomal protein per mL.<sup>c</sup> CL<sub>int(liver)</sub>: CL<sub>int(mic)</sub> × mg microsomal protein/g liver weight × g liver weight/kg body weight.<sup>d</sup> NCF (no co-factor): No NADPH regenerating system is added to NCF samples during the 60 min incubation.

modes of **14l** with JAK2 and FLT3, a molecular docking was performed using Schrödinger Maestro Glide 4.5.208 (Fig. 8). As shown in Fig. 8A, **14l** bound to the ATP-binding pocket of JAK2 in a manner similar to Fedratinib (Fig. 8C). Two hydrogen bonds were formed between the 2-aminopyrimidine moiety of **14l** and hinge residues LEU932; meanwhile the 6-chloro pyrimidine group together with adjacent residues (e.g., VAL863, ALA880, VAL911, MET929 and LEU983) composed net-like hydrophobic interactions. Besides, the morpholine moiety formed a hydrogen bond with LYS943 which exposed in the solvent area, and another two hydrogen bonds were formed between the tail carbonyl group with ASP976 and ARG980.

In Fig. 8B, we also found the configuration of **14l** resembled that of Fedratinib. Two hydrogen bonds were observed between 2-aminopyrimidine moiety and CYS694. LYS650 formed a hydrogen bond with the carbonyl group of piperazine urea fragment in **14l** and the sulfonyl group of sulfonamide fragment in Fedratinib, respectively. Strong hydrophobic interactions also existed between 6-chloro pyrimidine structure and the hydrophobic cavity of FLT3 (related residues are ALA648, VAL675 and PHE691). Besides, the hydrogen bond between the carbonyl group of **14l** and SER624 was not observed in Fedratinib, which might explain that **14l** exerted higher FLT3 activity than Fedratinib.

### 3. Conclusion

We have presented the discovery of a series of 2-aminopyrimidine derivatives as potent inhibitors targeting JAK2 and FLT3. Starting from compound **3**, step-by-step lead optimization was carried out based on SAR studies with the help of CADD, and a focused library of compounds was prepared. Among them, compound **14l** was discovered as the most potent JAK2/FLT3 dual inhibitor with IC<sub>50</sub> values of 1.8 nM and 0.68 nM, respectively. **14l** also exerted good anti-proliferative activities to HEL and Molm-13 with IC<sub>50</sub> values of 0.84 μM and 0.019 μM, respectively. Remarkably, **14l** showed less cytotoxicity against JAK2/FLT3-independent cells than Pacritinib and Fedratinib, which may indicated a better safety profile. Also, **14l** exhibited moderate metabolic stability in the RLM assay and certain selectivity among 20 different common tyrosine kinases. Furthermore, flow cytometry showed that **14l** was able to block the G<sub>1</sub>/S cell cycle, triggered apoptosis of Molm-13 cells in a dose-dependent manner. In conclusion, we suggest compound **14l** to be a promising JAK2/FLT3 inhibitor and worthy of further development.

### 4. Experimental section

#### 4.1. Chemistry

Unless otherwise specified, reagents and solvents were purchased from commercial suppliers and used without further purification. The termination time of reactions was monitored on silica gel plates with fluorescent indicator 254 nm. Flash column chromatography was run on

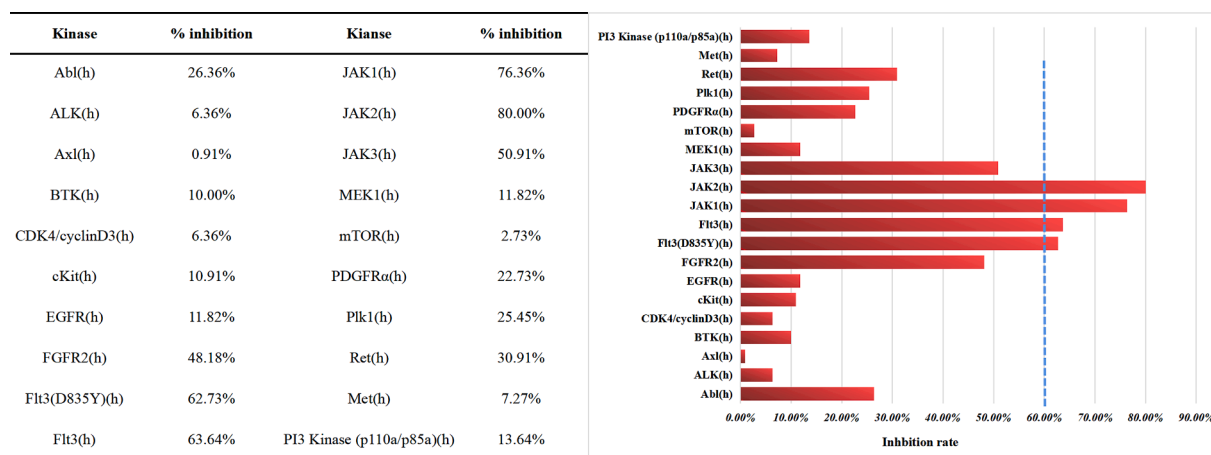


**Fig. 5.** Selectivity profiles of compound 141 measured at a concentration of 30 nM in a panel of 20 kinases generated with the KINOMEScan® Kinase Profiling Service from Eurofins Discovery. The results represent the mean of two independent experiments performed in duplicate.

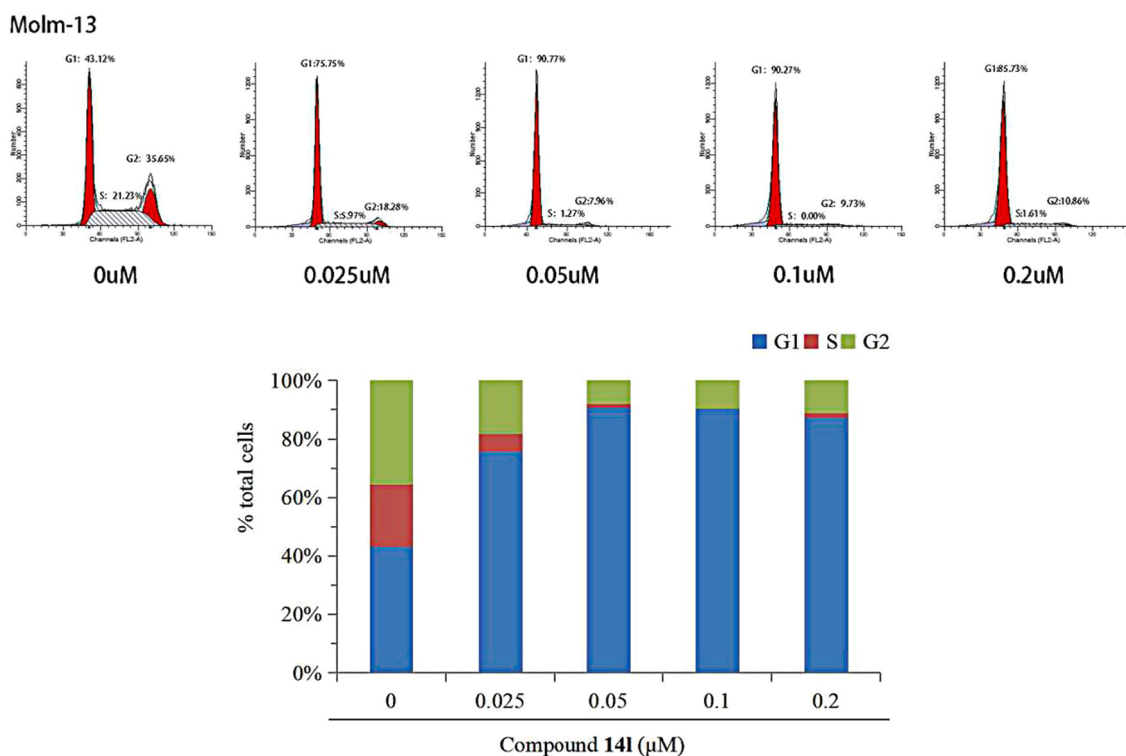


**Fig. 6.** After a 48 h treatment, compound 141 induced dose-dependent cell cycle G<sub>1</sub>/S phase arrest in Molm-13 cells.

silica gel (200–300 mesh) from Qingdao Ocean Chemicals (Qingdao, Shandong, China). Mass spectra (MS) were obtained using Agilent 1100 LC-MS (Agilent, Palo Alto, CA, USA). The purities of biologically evaluated compounds were > 95% as determined by HPLC. All melting points were determined on a Mettler Melting Point MP70 apparatus (Mettler, Toledo, Switzerland) without calibration. <sup>1</sup>H NMR and <sup>13</sup>C NMR spectra were performed on a Bruker spectrometers (Bruker Bioscience, respectively, Billerica, MA, USA) with TMS as an internal standard.

Fedratinib (**1**) was synthesized refer to patent WO2007053452. <sup>1</sup>H NMR (600 MHz, DMSO)  $\delta$  8.78 (s, 1H), 8.55 (s, 1H), 8.13 (d,  $J$  = 5.4 Hz, 2H), 7.90 (s, 1H), 7.57 (s, 1H), 7.53 (d,  $J$  = 9.0 Hz, 2H), 7.49 (dd,  $J$  = 4.8, 2.4 Hz, 2H), 6.80 (d,  $J$  = 9.1 Hz, 2H), 4.00 (t,  $J$  = 6.0 Hz, 2H), 2.77 (t,  $J$  = 5.9 Hz, 2H), 2.53 (s, 4H), 2.12 (s, 3H), 1.70–1.67 (m, 4H), 1.12 (s, 10H). <sup>13</sup>C NMR (151 MHz, DMSO)  $\delta$  159.43, 158.75, 156.55, 153.35,

144.87, 140.99, 134.69, 129.31, 125.31, 120.77, 120.47, 119.42, 114.71, 106.06, 67.21, 54.88, 54.46, 53.67, 30.25, 23.60, 13.98. m.p.: 176.6–178.3 °C. HPLC purity: 96.89%, retention time = 13.767 min. LC-MS (ESI positive mode)  $m/z$  525.08 ([M+H]<sup>+</sup>).

Pacritinib (**2**) was purchased from Shanghai Bide Pharmatech Ltd. (Shanghai, China, HPLC purity > 97%).

#### 4.1.1. Preparation of intermediates 5a-m

**4.1.1.1. tert-butyl 4-(2-chloro-5-methylpyrimidin-4-yl)piperazine-1-carboxylate (5a).** **General procedure A:** 6.5 g of *N*-Boc-piperazine (35.2 mmol) in 50 mL DMF was stirred in –10 °C for 10 min, then 5.0 g of 2,4-dichloro-5-methylpyrimidine (30.9 mmol) and 5.5 mL of Et<sub>3</sub>N (40.2 mmol) in 50 mL DMF was added dropwise below 0 °C. The mixture was stirred at room temperature for 4 h. The resulting mixture was

## Molm-13

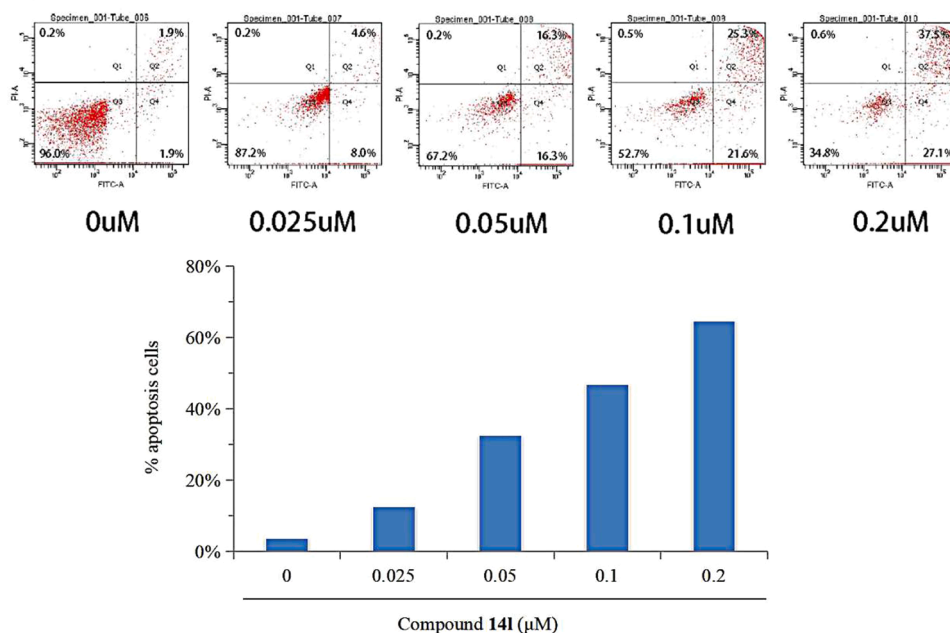


Fig. 7. After a 48 h treatment, compound 141 induced dose-dependent apoptosis in Molm-13 cells.

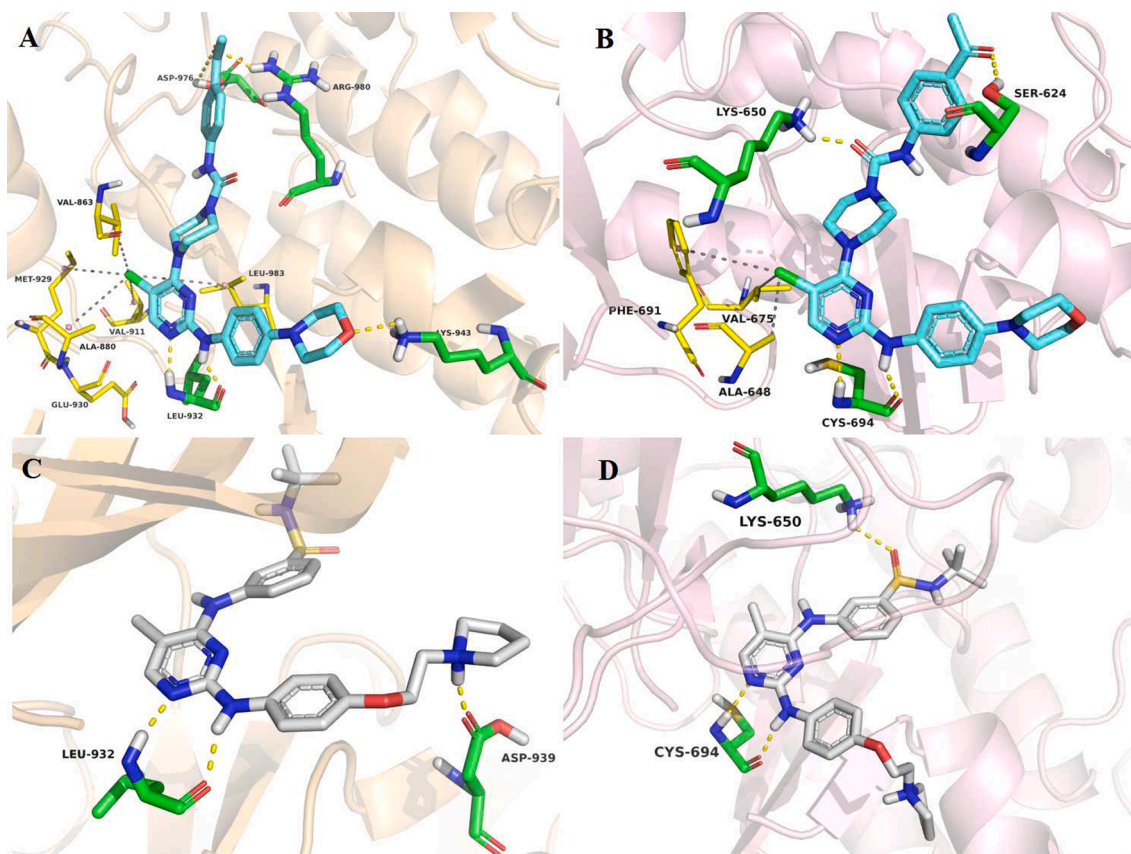


Fig. 8. Binding mode examination of compound 141 (blue) and Fedratinib (white); hydrogen bonds are shown as yellow dashes; hydrophobic interactions are shown as grey dashes. (A) Docking of 141 into JAK2 kinase (PDB code 4J19). (B) Docking of 141 into the homology model of FLT3 kinase. (C) Docking of Fedratinib into JAK2 kinase (PDB code 4J19). (D) Docking of Fedratinib into the homology model of FLT3 kinase. (For interpretation of the references to colour in this figure legend, the reader is referred to the web version of this article.)

poured into ice-water (200 mL) and stirred for 30 min, then the precipitate was filtered and dried in vacuum. Using PE/EA (1:1) as eluent to purify crude product by flash column chromatography, 7.2 g of **5a** was obtained. White solid; yield: 75.0%. LC-MS (ESI positive mode)  $m/z$  313.23 ( $[M+H]^+$ ).

**4.1.1.2. tert-butyl 4-(2-chloro-6-methylpyrimidin-4-yl)piperazine-1-carboxylate (5b).** 0.8 g of **5b** was obtained followed by the **general procedure A**, 0.5 g (3.1 mmol) of 2,4-dichloro-6-methylpyrimidine, 0.7 g (3.7 mmol) of *N*-Boc-piperazine and 0.6 mL of Et<sub>3</sub>N (4.1 mmol) were used. White solid; yield: 83.3%. LC-MS (ESI positive mode)  $m/z$  313.22 ( $[M+H]^+$ ).

**4.1.1.3. tert-butyl 4-(2-chlorothieno[3,2-d]pyrimidin-4-yl)piperazine-1-carboxylate (5c).** 0.75 g of **5c** was obtained followed by the **general procedure A**, 0.5 g (2.45 mmol) of 2,4-dichlorothieno[3,2-d]pyrimidine, 0.55 g (2.94 mmol) of *N*-Boc-piperazine and 0.45 mL of Et<sub>3</sub>N (3.19 mmol) were used. White solid; yield: 86.2%. LC-MS (ESI positive mode)  $m/z$  355.02 ( $[M+H]^+$ ).

**4.1.1.4. tert-butyl 4-(2-chloroquinazolin-4-yl)piperazine-1-carboxylate (5d).** 0.74 g of **5d** was obtained followed by the **general procedure A**, 0.5 g (2.53 mmol) of 2,4-dichloroquinazoline, 0.56 g (3.03 mmol) of *N*-Boc-piperazine and 0.46 mL of Et<sub>3</sub>N (3.29 mmol) were used. White solid; yield: 84.1%. LC-MS (ESI positive mode)  $m/z$  349.41 ( $[M+H]^+$ ).

**4.1.1.5. tert-butyl 4-(2-chloro-5-fluoropyrimidin-4-yl)piperazine-1-carboxylate (5e).** 0.78 g of **5e** was obtained followed by the **general procedure A**, 0.5 g (3.0 mmol) of 2,4-dichloro-5-fluoropyrimidine, 0.67 g (3.6 mmol) of *N*-Boc-piperazine and 0.58 mL of Et<sub>3</sub>N (4.0 mmol) were used. White solid; yield: 82.1%. LC-MS (ESI positive mode)  $m/z$  317.10 ( $[M+H]^+$ ).

**4.1.1.6. tert-butyl 4-(2,5-dichloropyrimidin-4-yl)piperazine-1-carboxylate (5f).** 0.82 g of **5f** was obtained followed by the **general procedure A**, 0.5 g (2.75 mmol) of 2,4,5-trichloropyrimidine, 0.61 g (3.3 mmol) of *N*-Boc-piperazine and 0.51 mL of Et<sub>3</sub>N (3.5 mmol) were used. White solid; yield: 90.1%. LC-MS (ESI positive mode)  $m/z$  333.28 ( $[M+H]^+$ ).

**4.1.1.7. tert-butyl 4-(2-chloro-5-(trifluoromethyl)pyrimidin-4-yl)piperazine-1-carboxylate (5g).** 0.68 g of **5g** was obtained followed by the **general procedure A**, 0.5 g (2.31 mmol) of 2,4-dichloro-5-(trifluoromethyl)pyrimidine, 0.52 g (2.78 mmol) of *N*-Boc-piperazine and 0.43 mL of Et<sub>3</sub>N (3.01 mmol) were used. White solid; yield: 80.3%. LC-MS (ESI positive mode)  $m/z$  367.42 ( $[M+H]^+$ ).

**4.1.1.8. tert-butyl 4-(2-chloro-5-nitropyrimidin-4-yl)piperazine-1-carboxylate (5h).** 0.76 g of **5h** was obtained followed by the **general procedure A**, 0.5 g (2.60 mmol) of 2,4-dichloro-5-nitropyrimidine, 0.58 g (3.11 mmol) of *N*-Boc-piperazine and 0.48 mL of Et<sub>3</sub>N (3.36 mmol) were used. Yellow solid; yield: 85.4%. LC-MS (ESI positive mode)  $m/z$  344.02 ( $[M+H]^+$ ).

**4.1.1.9. tert-butyl 4-((2-chloro-5-nitropyrimidin-4-yl)amino)piperidine-1-carboxylate (5i).** 0.84 g of **5i** was obtained followed by the **general procedure A**, 0.5 g (2.60 mmol) of 2,4-dichloro-5-nitropyrimidine, 0.62 g (3.12 mmol) of *tert*-butyl 4-aminopiperidine and 0.48 mL of Et<sub>3</sub>N (3.36 mmol) were used. Yellow solid; yield: 90.3%. LC-MS (ESI positive mode)  $m/z$  358.22 ( $[M+H]^+$ ).

**4.1.1.10. Ethyl 1-(2-chloro-5-methylpyrimidin-4-yl)piperidine-4-carboxylate (5j).** 0.75 g of **5j** was obtained followed by the **general procedure A**, 0.5 g (3.1 mmol) of 2,4-dichloro-5-methylpyrimidine, 0.53 g (3.72 mmol) of ethyl piperidine-4-carboxylate and 0.6 mL of Et<sub>3</sub>N (4.1 mmol) were used. White solid; yield: 90.3%. LC-MS (ESI positive mode)  $m/z$

284.40 ( $[M+H]^+$ ).

**4.1.1.11. tert-butyl 3-((2-chloro-5-methylpyrimidin-4-yl)amino)azetidine-1-carboxylate (5k).** 0.83 g of **5k** was obtained followed by the **general procedure A**, 0.5 g (3.1 mmol) of 2,4-dichloro-5-methylpyrimidine, 0.64 g (3.72 mmol) of *tert*-butyl 3-aminoazetidine-1-carboxylate and 0.6 mL of Et<sub>3</sub>N (4.1 mmol) were used. White solid; yield: 90.2%. LC-MS (ESI positive mode)  $m/z$  299.43 ( $[M+H]^+$ ).

**4.1.1.12. tert-butyl 3-((2-chloro-5-methylpyrimidin-4-yl)amino)pyrrolidine-1-carboxylate (5l).** 0.84 g of **5l** was obtained followed by the **general procedure A**, 0.5 g (3.1 mmol) of 2,4-dichloro-5-methylpyrimidine, 0.69 g (3.72 mmol) of *tert*-butyl 3-aminopyrrolidine-1-carboxylate and 0.6 mL of Et<sub>3</sub>N (4.1 mmol) were used. White solid; yield: 84.4%. LC-MS (ESI positive mode)  $m/z$  313.16 ( $[M+H]^+$ ).

**4.1.1.13. tert-butyl 4-((2-chloro-5-methylpyrimidin-4-yl)amino)piperidine-1-carboxylate (5m).** 0.86 g of **5m** was obtained followed by the **general procedure A**, 0.5 g (3.1 mmol) of 2,4-dichloro-5-methylpyrimidine, 0.74 g (3.72 mmol) of *tert*-butyl 4-aminopiperidine-1-carboxylate and 0.6 mL of Et<sub>3</sub>N (4.1 mmol) were used. White solid; yield: 85.1%. LC-MS (ESI positive mode)  $m/z$  327.19 ( $[M+H]^+$ ).

#### 4.1.2. Preparation of intermediates **6a-m**

**4.1.2.1. tert-butyl 4-(5-methyl-2-((4-morpholinophenyl)amino)pyrimidin-4-yl)piperazine-1-carboxylate (6a).** **General procedure B:** To a solution of **5a** (5.0 g, 16.0 mmol) and trifluoroacetate (5.47 g, 48.0 mmol) in 50 mL *i*-PrOH, 4-morpholinoaniline (3.4 g, 19.2 mmol) was added and the resulted mixture was stirred at 100 °C for 1 h in the sealed-tube. The mixture was poured into 100 mL ice water, after neutralized by 10% NaOH, the precipitate formed and filtered, washed with water and dried in vacuum to afford crude product **6a** without further purification. LC-MS (ESI positive mode)  $m/z$  455.32 ( $[M+H]^+$ ).

**4.1.2.2. tert-butyl 4-(6-methyl-2-((4-morpholinophenyl)amino)pyrimidin-4-yl)piperazine-1-carboxylate (6b).** Crude **6b** was obtained followed by the **general procedure B**, 0.6 g (1.9 mmol) of **5b**, 0.65 g (5.7 mmol) of trifluoroacetate and 0.41 g (2.28 mmol) of 4-morpholinoaniline were used. LC-MS (ESI positive mode)  $m/z$  455.32 ( $[M+H]^+$ ).

**4.1.2.3. tert-butyl 4-(2-((4-morpholinophenyl)amino)thieno[3,2-d]pyrimidin-4-yl)piperazine-1-carboxylate (6c).** Crude **6c** was obtained followed by the **general procedure B**, 0.6 g (1.7 mmol) of **5c**, 0.58 g (5.1 mmol) of trifluoroacetate and 0.36 g (2.04 mmol) of 4-morpholinoaniline were used. LC-MS (ESI positive mode)  $m/z$  497.08 ( $[M+H]^+$ ).

**4.1.2.4. tert-butyl 4-(2-((4-morpholinophenyl)amino)quinazolin-4-yl)piperazine-1-carboxylate (6d).** Crude **6d** was obtained followed by the **general procedure B**, 0.6 g (1.72 mmol) of **5d**, 0.59 g (5.2 mmol) of trifluoroacetate and 0.37 g (2.06 mmol) of 4-morpholinoaniline were used. LC-MS (ESI positive mode)  $m/z$  491.06 ( $[M+H]^+$ ).

**4.1.2.5. tert-butyl 4-(5-fluoro-2-((4-morpholinophenyl)amino)pyrimidin-4-yl)piperazine-1-carboxylate (6e).** Crude **6e** was obtained followed by the **general procedure B**, 0.6 g (1.9 mmol) of **5e**, 0.65 g (5.7 mmol) of trifluoroacetate and 0.41 g (2.28 mmol) of 4-morpholinoaniline were used. LC-MS (ESI positive mode)  $m/z$  459.31 ( $[M+H]^+$ ).

**4.1.2.6. tert-butyl 4-(5-chloro-2-((4-morpholinophenyl)amino)pyrimidin-4-yl)piperazine-1-carboxylate (6f).** Crude **6f** was obtained followed by the **general procedure B**, 0.6 g (1.81 mmol) of **5f**, 0.62 g (5.4 mmol) of trifluoroacetate and 0.39 g (2.17 mmol) of 4-morpholinoaniline were used. LC-MS (ESI positive mode)  $m/z$  475.25 ( $[M+H]^+$ ).

4.1.2.7. *tert-butyl-4-(2-((4-morpholinophenyl)amino)-5-(trifluoromethyl)pyrimidin-4-yl)piperazine-1-carboxylate (6g)*. Crude **6g** was obtained followed by the **general procedure B**, 0.6 g (1.64 mmol) of **5g**, 0.56 g (4.9 mmol) of trifluoroacetate and 0.35 g (1.97 mmol) of 4-morpholinoaniline were used. LC-MS (ESI positive mode)  $m/z$  509.10 ( $[M+H]^+$ ).

4.1.2.8. *tert-butyl-4-(2-((4-morpholinophenyl)amino)-5-nitropyrimidin-4-yl)piperazine-1-carboxylate (6h)*. Crude **6h** was obtained followed by the **general procedure B**, 0.6 g (1.75 mmol) of **5h**, 0.60 g (5.2 mmol) of trifluoroacetate and 0.37 g (2.1 mmol) of 4-morpholinoaniline were used. LC-MS (ESI positive mode)  $m/z$  486.07 ( $[M+H]^+$ ).

4.1.2.9. *tert-butyl-4-(2-((4-morpholinophenyl)amino)-5-nitropyrimidin-4-yl)amino)piperidine-1-carboxylate (6i)*. Crude **6i** was obtained followed by the **general procedure B**, 0.6 g (1.68 mmol) of **5i**, 0.57 g (5.04 mmol) of trifluoroacetate and 0.36 g (2.04 mmol) of 4-morpholinoaniline were used. LC-MS (ESI positive mode)  $m/z$  500.02 ( $[M+H]^+$ ).

4.1.2.10. *ethyl-1-(5-methyl-2-((4-morpholinophenyl)amino)pyrimidin-4-yl)piperidine-4-carboxylate (6j)*. Crude **6j** was obtained followed by the **general procedure B**, 0.6 g (2.1 mmol) of **5c** and 0.73 g (6.36 mmol) of trifluoroacetate and 0.45 g (2.54 mmol) of 4-morpholinoaniline in 6 mL of *i*-PrOH, crude product of and directly used without purification. LC-MS (ESI positive mode)  $m/z$  426.44 ( $[M+H]^+$ ).

4.1.2.11. *N-(azetid-3-yl)-2-chloro-5-methyl-pyrimidine-4-amine hydrochloride (6k)*. **General procedure C**: 0.6 g (2.01 mmol) of **5k** was added to 6 mL of ethyl acetate hydrochloride solution (4 M). After reacted for 12 h at room temperature, gray precipitate formed and filtered, washed with ethyl acetate and dried in vacuum to afford crude product **6k** without further purification. LC-MS (ESI positive mode)  $m/z$  199.14 ( $[M+H]^+$ ).

4.1.2.12. *2-chloro-5-methyl-N-(pyrrolidin-3-yl)pyrimidin-4-amine hydrochloride (6l)*. Crude **6l** was obtained followed by the **general procedure C**, 0.6 g (1.92 mmol) of **5l** and 6 mL of ethyl acetate hydrochloride solution (4 M) were used. LC-MS (ESI positive mode)  $m/z$  213.31 ( $[M+H]^+$ ).

4.1.2.13. *2-chloro-5-methyl-N-(piperidin-4-yl)pyrimidin-4-amine hydrochloride (6m)*. Crude **6m** was obtained followed by the **general procedure C**, 0.6 g (1.84 mmol) of **5m** and 6 mL of ethyl acetate hydrochloride solution (4 M) were used. LC-MS (ESI positive mode)  $m/z$  227.33 ( $[M+H]^+$ ).

#### 4.1.3. Preparation of compounds 7a-n

4.1.3.1. *5-methyl-N-(4-morpholinophenyl)-4-(piperazin-1-yl)pyrimidin-2-amine (7a)*. **General procedure D**: The crude **6a** was added to a mixture of 30 mL of DCM and 30 mL of TFA, after stirring at room temperature overnight, the solvent was evaporated and the resultant was added to 60 mL water, the pH was adjusted to 8 with saturated  $\text{NaHCO}_3$ , the precipitate formed and filtered, washed with water and dried in vacuum to afford 4.6 g of **7a**. Grey solid; yield: 80.7%. LC-MS (ESI positive mode)  $m/z$  355.05 ( $[M+H]^+$ ).

4.1.3.2. *4-methyl-N-(4-morpholinophenyl)-6-(piperazin-1-yl)pyrimidin-2-amine (7b)*. 0.51 g of **7b** was obtained followed by the **general procedure D**, 6 mL of DCM and 6 mL of TFA were used; yield: 75%. LC-MS (ESI positive mode)  $m/z$  355.06 ( $[M+H]^+$ ).

4.1.3.3. *N-(4-morpholinophenyl)-4-(piperazin-1-yl)thieno[3,2-d]pyrimidin-2-amine (7c)*. 0.56 g of **7c** was obtained followed by the **general procedure D**, 6 mL of DCM and 6 mL of TFA were used; yield: 83.5%. LC-MS (ESI positive mode)  $m/z$  343.02 ( $[M+H]^+$ ). LC-MS (ESI positive

mode)  $m/z$  397.21 ( $[M+H]^+$ ).

4.1.3.4. *N-(4-morpholinophenyl)-4-(piperazin-1-yl)quinazolin-2-amine (7d)*. 0.53 g of **7d** were obtained followed by the **general procedure D**, 6 mL of DCM and 6 mL of TFA were used; yield: 79.1%. LC-MS (ESI positive mode)  $m/z$  391.16 ( $[M+H]^+$ ).

4.1.3.5. *5-fluoro-N-(4-morpholinophenyl)-4-(piperazin-1-yl)pyrimidin-2-amine (7e)*. 0.54 g of **7e** were obtained followed by the **general procedure D**, 6 mL of DCM and 6 mL of TFA were used; yield: 79.4%. LC-MS (ESI positive mode)  $m/z$  359.26 ( $[M+H]^+$ ).

4.1.3.6. *5-chloro-N-(4-morpholinophenyl)-4-(piperazin-1-yl)pyrimidin-2-amine (7f)*. 0.52 g of **7f** were obtained followed by the **general procedure D**, 6 mL of DCM and 6 mL of TFA were used; yield: 77.3%. LC-MS (ESI positive mode)  $m/z$  375.01 ( $[M+H]^+$ ).

4.1.3.7. *N-(4-morpholinophenyl)-4-(piperazin-1-yl)-5-(trifluoromethyl)pyrimidin-2-amine (7g)*. 0.49 g of **7g** were obtained followed by the **general procedure D**, 6 mL of DCM and 6 mL of trifluoroacetate were used; yield: 73.1%. LC-MS (ESI positive mode)  $m/z$  409.36 ( $[M+H]^+$ ).

4.1.3.8. *N-(4-morpholinophenyl)-5-nitro-4-(piperazin-1-yl)pyrimidin-2-amine (7h)*. 0.50 g of **7h** were obtained followed by the **general procedure D**, 6 mL of DCM and 6 mL of TFA were used; yield: 74.6%. LC-MS (ESI positive mode)  $m/z$  386.14 ( $[M+H]^+$ ).

4.1.3.9. *tert-butyl-4-((5-amino-2-((4-morpholinophenyl)amino)pyrimidin-4-yl)amino)piperidine-1-carboxylate (7i)*. To a solution of **6i** in ethanol (10 mL), 0.1 g of Pd-C (10% m/m) was added and hydrogenated at room temperature for 12 h. After filtration, the filtrate was concentrated to afford 0.6 g of **7i** as purple solid; yield: 76.9%. LC-MS (ESI positive mode)  $m/z$  470.11 ( $[M+H]^+$ ).

4.1.3.10. *1-(5-methyl-2-((4-morpholinophenyl)amino)pyrimidin-4-yl)piperidine-4-carboxylic acid (7j)*. The crude **6j** was dissolved in a mixture of 10 mL MeOH and 10 mL (1 M) sodium hydroxide solution, the resulted mixture was stirred at 60 °C for 2 h. Then, the solvent was evaporated and added the resultant to 10 mL water; pH of mixture was adjusted to 3 with 10% hydrochloric acid. White precipitate was filtered and dried in vacuum to afford 0.63 g of **7j**. Pale yellow solid; yield: 75%. LC-MS (ESI positive mode)  $m/z$  398.13 ( $[M+H]^+$ ).

4.1.3.11. *N-(4-acetylphenyl)-3-((2-chloro-5-methylpyrimidin-4-yl)amino)azetid-1-carboxamide (7k)*. **General procedure E**: 0.25 g of **6k** (1.07 mmol) and 0.7 g of DIPEA (5.37 mmol) were dissolved in 5 mL DMF, after addition of phenyl *N*-(4-acetylphenyl)carbamate (0.32 g, 1.28 mmol), the resulted mixture was stirred at 40 °C for 12 h. The mixture was added to 10 mL ice-water, then the pink precipitate formed and filtered, washed with water and dried in vacuum. was by flash column chromatography Using DCM/MeOH (20:1) as eluent to further purify the crude product, 0.26 g of **7k** was obtained. Pink solid; yield: 68.4%. LC-MS (ESI positive mode)  $m/z$  360.18 ( $[M+H]^+$ ).

4.1.3.12. *N-(4-acetylphenyl)-3-((2-chloro-5-methylpyrimidin-4-yl)amino)pyrrolidine-1-carboxamide (7l)*. 0.50 g of **7l** was obtained followed by the **general procedure E**, 0.4 g (1.61 mmol) of **6l**, 1.04 g (8.06 mmol) of DIPEA and 0.49 g (1.27 mmol) of Phenyl *N*-(4-acetylphenyl)carbamate were used. Purple solid; yield: 83.3%. LC-MS (ESI positive mode)  $m/z$  374.21 ( $[M+H]^+$ ).

4.1.3.13. *N-(4-acetylphenyl)-4-((2-chloro-5-methylpyrimidin-4-yl)amino)piperidine-1-carboxamide (7m)*. 0.23 g of **7m** was obtained followed by the **general procedure E**, 0.25 g (0.95 mmol) of **6m**, 0.61 g (4.75 mmol) of DIPEA and 0.29 g (1.14 mmol) of Phenyl *N*-(4-acetylphenyl)

carbamate were used. Blue solid; yield: 62.6%. LC-MS (ESI positive mode)  $m/z$  388.17 ( $[M+H]^+$ ).

#### 4.1.3.14. 1-(4-(2-chloro-5-methylpyrimidin-4-yl)amino)piperidin-1-yl)ethan-1-one. (7n)

**General procedure F:** 0.25 g of **6m** (0.95 mmol) and 0.2 mL of Et<sub>3</sub>N (1.43 mmol) were dissolved in 5 mL DCM, 0.14 g of acetyl chloride (1.82 mmol) was added and the mixture was stirred at room temperature for 4 h. The mixture was evaporated and the resultant was added to 10 mL water, then the gray precipitate formed and filtered. Using DCM/MeOH (20:1) as eluent to further purify the crude product by flash column chromatography, 0.21 g of **7n** was obtained. Gray solid; yield: 82.3%. LC-MS (ESI positive mode)  $m/z$  269.40 ( $[M+H]^+$ ).

#### 4.1.4. Preparation of intermediate 8

To a mixture of **7i** (0.6 g, 1.27 mmol) and HOAc (0.08 g, 0.13 mmol) in 20 mL EtOH, formic propionic anhydride (0.14 g, 1.4 mmol) was added and the resulted mixture was heated to 80 °C and stirred for 5 h. After the evaporation of mixture under reduced pressure, the resultant was poured to 20 mL water, the precipitate was collected after filtration and dryness in vacuum. 0.58 g of **8** as grey solid was obtained; yield: 89.2%. LC-MS (ESI positive mode)  $m/z$  508.12 ( $[M+H]^+$ ).

#### 4.1.5. Preparation of intermediate 9

0.43 g of **9** was obtained followed by the **general procedure D**, 6 mL of DCM and 6 mL of TFA were used. Green solid; yield: 91.5%. LC-MS (ESI positive mode)  $m/z$  408.30 ( $[M+H]^+$ ).

#### 4.1.6. Preparation of intermediates 11a-b

**4.1.6.1. tert-butyl 3-(3-(4-acetylphenyl)ureido)azetidine-1-carboxylate (11a).** 0.56 g of **11a** was obtained followed by the **general procedure E**, 0.41 g of *tert*-butyl 3-aminoazetidine-1-carboxylate (2.35 mmol), 0.5 g of phenyl *N*-(4-acetylphenyl)carbamate (1.96 mmol) and 0.75 g of DIPEA (5.88 mmol) were used. White solid; yield: 86.1%. LC-MS (ESI positive mode)  $m/z$  334.05 ( $[M+H]^+$ ).

**4.1.6.2. tert-butyl 3-(3-(4-acetylphenyl)ureido)pyrrolidine-1-carboxylate (11b).** 0.58 g of **11b** was obtained followed by the **general procedure E**, 0.44 g (2.35 mmol) of *tert*-butyl 3-aminopyrrolidine-1-carboxylate, 0.5 g (1.96 mmol) of phenyl (4-acetylphenyl)carbamate and 0.75 g (5.88 mmol) of DIPEA were used. White solid; yield: 85.2%. LC-MS (ESI positive mode)  $m/z$  348.31 ( $[M+H]^+$ ).

#### 4.1.7. Preparation of intermediates 12a-b

**4.1.7.1. 1-(4-acetylphenyl)-3-(azetidin-3-yl)urea hydrochloride (12a).** Crude **12a** was obtained followed by the **general procedure C**, 0.56 g (1.68 mmol) of **11a** and 6 mL of ethyl acetate hydrochloride solution (4 M) were used. LC-MS (ESI positive mode)  $m/z$  234.05 ( $[M+H]^+$ ).

**4.1.7.2. 1-(4-acetylphenyl)-3-(pyrrolidin-3-yl)urea hydrochloride (12b).** Crude **12b** was obtained followed by the **general procedure C**, 0.58 g (1.67 mmol) of **11b** and 6 mL of ethyl acetate hydrochloride solution (4 M) were used. LC-MS (ESI positive mode)  $m/z$  248.10 ( $[M+H]^+$ ).

#### 4.1.8. Preparation of intermediates 13a-b

**4.1.8.1. 1-(4-acetylphenyl)-3-(1-(2-chloro-5-methylpyrimidin-4-yl)azetidin-3-yl)urea (13a).** 0.38 g of **13a** was obtained followed by the **general procedure A**, 0.4 g of **12a** (1.47 mmol), 0.2 g of 2,4-dichloro-5-methylpyrimidine (1.23 mmol) and 0.5 mL of Et<sub>3</sub>N (3.7 mmol) were used. White solid; yield: 86.4%. LC-MS (ESI positive mode)  $m/z$  359.95 ( $[M+H]^+$ ).

**4.1.8.2. 1-(4-acetylphenyl)-3-(1-(2-chloro-5-methylpyrimidin-4-yl)pyrrolidin-3-yl)urea (13b).** 0.35 g of **13b** was obtained followed by the **general procedure A**, 0.2 g (1.23 mmol) of 2,4-dichloro-5-methylpyrimidine, 0.42 g (1.47 mmol) of **12b** and 0.5 mL of Et<sub>3</sub>N (3.7 mmol) were used. White solid; yield: 77.8%. LC-MS (ESI positive mode)  $m/z$  374.03 ( $[M+H]^+$ ).

#### 4.1.9. Preparation of compounds (14a-o, 15a-h, 16a-h)

**4.1.9.1. N-(4-acetylphenyl)-4-(5-methyl-2-((4-morpholinophenyl)amino)pyrimidin-4-yl)piperazine-1-carboxamide (14a).** Followed by the **general procedure E**, compound **14a** as white solid was obtained. <sup>1</sup>H NMR (600 MHz, DMSO)  $\delta$  9.00 (s, 1H), 8.87 (s, 1H), 7.90 (s, 1H), 7.88 (d,  $J$  = 8.7 Hz, 2H), 7.65 (d,  $J$  = 8.7 Hz, 2H), 7.59 (d,  $J$  = 9.0 Hz, 2H), 6.86 (d,  $J$  = 9.0 Hz, 2H), 3.74 – 3.71 (m, 4H), 3.65 – 3.60 (m, 4H), 3.47 – 3.42 (m, 4H), 3.02 – 2.98 (m, 4H), 2.12 (s, 3H). <sup>13</sup>C NMR (151 MHz, DMSO)  $\delta$  196.82, 164.96, 159.20, 158.71, 155.00, 145.95, 145.79, 134.30, 130.75, 129.68, 119.98, 118.66, 116.17, 107.89, 66.67, 49.92, 47.47, 44.18, 26.79, 16.62. m.p.: 248.1 – 252.2 °C. HPLC purity: 98.53%, retention time = 17.724 min. LC-MS (ESI positive mode)  $m/z$  516.11 ( $[M+H]^+$ ).

**4.1.9.2. N-(4-cyanophenyl)-4-(5-methyl-2-((4-morpholinophenyl)amino)pyrimidin-4-yl)piperazine-1-carboxamide (14b).** Followed by the **general procedure E**, compound **14b** as white solid was obtained. <sup>1</sup>H NMR (600 MHz, DMSO)  $\delta$  9.09 (s, 1H), 8.86 (s, 1H), 7.90 (s, 1H), 7.69 (s, 4H), 7.58 (d,  $J$  = 9.0 Hz, 2H), 6.86 (d,  $J$  = 9.0 Hz, 2H), 3.84 – 3.67 (m, 4H), 3.67 – 3.55 (m, 4H), 3.54 – 3.39 (m, 4H), 3.11 – 2.91 (m, 4H), 2.12 (s, 3H). <sup>13</sup>C NMR (151 MHz, DMSO)  $\delta$  164.96, 159.23, 158.73, 154.84, 145.95, 145.65, 134.31, 133.33, 119.93, 119.45, 116.17, 107.90, 103.51, 66.67, 49.92, 47.43, 44.17, 16.61. m.p.: 275.6 – 277.9 °C. HPLC purity: 98.16%, retention time = 18.101 min. LC-MS (ESI positive mode)  $m/z$  499.09 ( $[M+H]^+$ ).

**4.1.9.3. N-(4-acetylphenyl)-4-(6-methyl-2-((4-morpholinophenyl)amino)pyrimidin-4-yl)piperazine-1-carboxamide (14c).** Followed by the **general procedure E**, compound **14c** as white solid was obtained. <sup>1</sup>H NMR (600 MHz, DMSO)  $\delta$  9.00 (s, 1H), 8.85 (s, 1H), 7.88 (d,  $J$  = 9.0 Hz, 2H), 7.65 (d,  $J$  = 9.0 Hz, 2H), 7.58 (d,  $J$  = 9.0 Hz, 2H), 6.86 (d,  $J$  = 9.0 Hz, 2H), 6.15 (s, 1H), 3.74 – 3.72 (m, 4H), 3.66 (s, 4H), 3.59 (dd,  $J$  = 6.1, 3.6 Hz, 4H), 3.02 – 3.00 (m, 4H), 2.19 (s, 3H). <sup>13</sup>C NMR (151 MHz, DMSO)  $\delta$  196.83, 165.88, 163.12, 159.66, 154.89, 146.04, 145.75, 134.20, 130.78, 129.68, 120.29, 118.67, 116.13, 93.44, 66.67, 49.89, 43.84, 26.79, 24.17. m.p.: 235.5 – 243.7 °C. HPLC purity: 98.25%, retention time = 17.823 min. LC-MS (ESI positive mode)  $m/z$  516.18 ( $[M+H]^+$ ).

**4.1.9.4. N-(4-cyanophenyl)-4-(6-methyl-2-((4-morpholinophenyl)amino)pyrimidin-4-yl)piperazine-1-carboxamide (14d).** Followed by the **general procedure E**, compound **14d** as white solid was obtained. <sup>1</sup>H NMR (600 MHz, DMSO)  $\delta$  9.09 (s, 1H), 8.84 (s, 1H), 7.70 (s, 4H), 7.58 (d,  $J$  = 9.0 Hz, 2H), 6.86 (d,  $J$  = 9.0 Hz, 2H), 6.15 (s, 1H), 3.74 – 3.72 (m, 4H), 3.65 (s, 4H), 3.60 – 3.57 (m, 4H), 3.03 – 2.99 (m, 4H), 2.19 (s, 3H). <sup>13</sup>C NMR (151 MHz, DMSO)  $\delta$  163.11, 159.68, 154.72, 146.03, 145.61, 134.21, 133.32, 120.28, 119.88, 119.47, 116.12, 103.54, 99.99, 93.43, 66.67, 56.49, 49.89, 43.86, 24.18, 19.02. m.p.: 163.7 – 167.6 °C. HPLC purity: 99.34%, retention time = 18.035 min. LC-MS (ESI positive mode)  $m/z$  499.12 ( $[M+H]^+$ ).

**4.1.9.5. 2-(4-acetylphenyl)-1-(4-(2-((4-morpholinophenyl)amino)thieno[3,2-d]pyrimidin-4-yl)piperazin-1-yl)ethan-1-one (14e).** Followed by the **general procedure E**, compound **14e** as white solid was obtained. <sup>1</sup>H NMR (600 MHz, DMSO)  $\delta$  9.01 (s, 1H), 8.86 (s, 1H), 8.06 (d,  $J$  = 5.4 Hz, 1H), 7.89 (d,  $J$  = 9.0 Hz, 2H), 7.66 (d,  $J$  = 9.0 Hz, 2H), 7.64 (d,  $J$  = 9.0 Hz, 2H), 7.19 (d,  $J$  = 6.0 Hz, 1H), 6.89 (d,  $J$  = 9.0 Hz, 2H), 4.00 – 3.96 (m, 4H), 3.75 – 3.73 (m, 4H), 3.71 – 3.68 (m, 4H), 3.03 – 3.01 (m, 4H),

2.51 (s, 3H).  $^{13}\text{C}$  NMR (151 MHz, DMSO)  $\delta$  196.83, 163.69, 158.34, 158.19, 154.85, 146.01, 145.71, 134.47, 133.61, 130.81, 129.70, 124.15, 120.26, 118.68, 116.19, 105.99, 66.68, 49.94, 45.68, 43.91, 26.80. m.p.: 242.5 – 243.4 °C. HPLC purity: 99.31%, retention time = 19.219 min. LC-MS (ESI positive mode)  $m/z$  558.11 ( $[\text{M}+\text{H}]^+$ ).

4.1.9.6. *N*-(4-(2-(4-(2-((4-morpholinophenyl)amino)thieno[3,2-d]pyrimidin-4-yl)piperazin-1-yl)-2-oxoethyl)benzotriazole) (14f). Followed by the **general procedure E**, compound **14f** as white solid was obtained.  $^1\text{H}$  NMR (600 MHz, DMSO)  $\delta$  9.10 (s, 1H), 8.86 (s, 1H), 8.06 (d,  $J = 6.0$  Hz, 1H), 7.71 (s, 4H), 7.63 (d,  $J = 9.0$  Hz, 2H), 7.19 (d,  $J = 5.4$  Hz, 1H), 6.89 (d,  $J = 9.0$  Hz, 2H), 4.00 – 3.96 (m, 4H), 3.75 – 3.73 (m, 9H), 3.71 – 3.68 (m, 4H), 3.04 – 3.01 (m, 4H).  $^{13}\text{C}$  NMR (151 MHz, DMSO)  $\delta$  163.62, 158.33, 158.15, 154.69, 146.03, 145.58, 134.43, 133.64, 133.34, 124.11, 120.29, 119.87, 119.48, 116.18, 106.00, 103.59, 66.67, 49.93, 45.64, 43.90. m.p.: 289.5 – 291.4 °C. HPLC purity: 95.92%, retention time = 19.370 min. LC-MS (ESI positive mode)  $m/z$  541.01 ( $[\text{M}+\text{H}]^+$ ).

4.1.9.7. *N*-(4-(2-(4-(2-((4-morpholinophenyl)amino)quinazolin-4-yl)piperazine-1-carboxamide) (14g). Followed by the **general procedure E**, compound **14g** as white solid was obtained.  $^1\text{H}$  NMR (600 MHz, DMSO)  $\delta$  9.09 (s, 1H), 9.05 (s, 1H), 7.89 (s, 1H), 7.87 (d,  $J = 8.4$  Hz, 2H), 7.75 (d,  $J = 7.8$  Hz, 2H), 7.66 (d,  $J = 8.4$  Hz, 2H), 7.62 (t,  $J = 7.8$  Hz, 1H), 7.48 (d,  $J = 7.8$  Hz, 1H), 7.19 (t,  $J = 7.2$  Hz, 1H), 6.90 (d,  $J = 9.0$  Hz, 2H), 3.76 – 3.71 (m, 13H), 3.06 – 3.02 (m, 4H), 2.51 (s, 3H).  $^{13}\text{C}$  NMR (151 MHz, DMSO)  $\delta$  196.84, 165.48, 156.42, 155.02, 146.29, 145.77, 134.05, 133.21, 130.78, 129.69, 125.93, 121.65, 120.47, 118.70, 116.10, 112.78, 66.67, 49.84, 49.62, 44.01, 26.80. m.p.: 268.6 – 270.3 °C. HPLC purity: 97.46%, retention time = 18.722 min. LC-MS (ESI positive mode)  $m/z$  552.15 ( $[\text{M}+\text{H}]^+$ ).

4.1.9.8. *N*-(4-(2-(4-(2-((4-morpholinophenyl)amino)quinazolin-4-yl)piperazine-1-carboxamide) (14h). Followed by the **general procedure E**, compound **14h** as white solid was obtained.  $^1\text{H}$  NMR (600 MHz, DMSO)  $\delta$  9.13 (s, 1H), 9.08 (s, 1H), 7.86 (d,  $J = 8.4$  Hz, 1H), 7.76 (d,  $J = 8.4$  Hz, 2H), 7.71 (s, 4H), 7.64 – 7.60 (m, 1H), 7.49 (d,  $J = 8.4$  Hz, 1H), 7.19 (t,  $J = 7.8$  Hz, 1H), 6.90 (d,  $J = 9.0$  Hz, 2H), 3.74 (d,  $J = 9.3$  Hz, 13H), 3.05 – 3.02 (m, 4H).  $^{13}\text{C}$  NMR (151 MHz, DMSO)  $\delta$  165.48, 156.47, 154.85, 153.96, 146.27, 145.63, 134.09, 133.33, 133.19, 126.26, 125.90, 121.62, 120.45, 119.88, 119.50, 116.10, 112.79, 103.55, 66.67, 49.84, 49.58, 44.01. m.p.: 278.3 – 281.3 °C. HPLC purity: 96.00%, retention time = 18.903 min. LC-MS (ESI positive mode)  $m/z$  535.13 ( $[\text{M}+\text{H}]^+$ ).

4.1.9.9. *N*-(4-(2-(4-(2-((4-morpholinophenyl)amino)-7-oxopteridin-8(7H)-yl)piperidine-1-carboxamide) (14i). Followed by the **general procedure E**, compound **14i** as white solid was obtained.  $^1\text{H}$  NMR (600 MHz, DMSO)  $\delta$  10.11 (s, 1H), 9.10 (s, 1H), 8.79 (s, 1H), 7.89 (d,  $J = 8.5$  Hz, 2H), 7.68 (d,  $J = 8.5$  Hz, 2H), 7.65 (m, 2H), 6.89 (m, 2H), 5.36 (s, 1H), 4.40 (m, 2H), 3.95 – 3.42 (m, 4H), 3.38 – 3.36 (m, 1H), 3.13 – 2.69 (m, 8H), 2.51 (s, 3H), 1.74 (m, 2H).  $^{13}\text{C}$  NMR (151 MHz, DMSO)  $\delta$  196.74, 159.76, 158.38, 157.12, 154.60, 150.33, 147.40, 145.95, 131.64, 130.54, 129.62, 121.10, 120.90, 118.41, 115.68, 66.30, 65.29, 49.11, 44.33, 40.44, 27.25, 26.72, 15.55. m.p.: 283.8 – 286.0 °C. HPLC purity: 98.21%, retention time = 21.594 min. LC-MS (ESI positive mode)  $m/z$  569.2 ( $[\text{M}+\text{H}]^+$ ).

4.1.9.10. *8*-(1-(2-(4-(2-((4-morpholinophenyl)amino)pteridin-7(8H)-one) (14j). Followed by the **general procedure E**, compound **14j** as white solid was obtained.  $^1\text{H}$  NMR (600 MHz, DMSO)  $\delta$  10.08 (s, 1H), 8.77 (s, 1H), 7.86 (s, 1H), 7.57 (d,  $J = 7.8$  Hz, 2H), 6.93 (d,  $J = 7.8$  Hz, 2H), 5.35 (s, 1H), 4.63 (d,  $J = 8.4$  Hz, 1H), 3.99 (d,  $J = 11.4$  Hz, 1H), 3.75 (t,  $J = 4.7$  Hz, 4H), 3.10 – 3.06 (m, 4H), 2.62 (d,  $J = 67.5$  Hz, 4H), 2.05 (s, 3H), 1.69 (s, 2H).  $^{13}\text{C}$  NMR (151 MHz, DMSO)  $\delta$  168.48, 159.82, 157.18, 147.61, 121.39, 121.14, 115.74, 66.59, 49.29, 46.26, 41.33,

27.88, 27.17, 21.98. m.p.: 260.0 – 264.1 °C. HPLC purity: 96.06%, retention time = 19.592 min. LC-MS (ESI positive mode)  $m/z$  450.03 ( $[\text{M}+\text{H}]^+$ ).

4.1.9.11. *N*-(4-(2-(4-(2-((4-morpholinophenyl)amino)pyrimidin-4-yl)piperazine-1-carboxamide) (14k). Followed by the **general procedure E**, compound **14j** as white solid was obtained.  $^1\text{H}$  NMR (600 MHz, DMSO)  $\delta$  9.00 (s, 1H), 8.96 (s, 1H), 8.00 (d,  $J = 6.6$  Hz, 1H), 7.88 (d,  $J = 9.0$  Hz, 2H), 7.64 (d,  $J = 8.4$  Hz, 2H), 7.52 (d,  $J = 9.0$  Hz, 2H), 6.87 (d,  $J = 9.0$  Hz, 2H), 3.75 – 3.72 (m, 9H), 3.64 – 3.61 (m, 4H), 3.03 – 3.00 (m, 4H), 2.51 (s, 4H).  $^{13}\text{C}$  NMR (151 MHz, DMSO)  $\delta$  196.83, 156.17, 154.87, 151.62, 146.24, 145.72, 144.09, 142.53, 140.92, 133.98, 130.79, 129.69, 120.20, 118.67, 116.10, 66.65, 49.84, 45.82, 43.95, 26.79. m.p.: 240.9 – 241.8 °C. HPLC purity: 97.55%, retention time = 20.127 min. LC-MS (ESI positive mode)  $m/z$  520.08 ( $[\text{M}+\text{H}]^+$ ).

4.1.9.12. *N*-(4-(2-(4-(2-((4-morpholinophenyl)amino)pyrimidin-4-yl)piperazine-1-carboxamide) (14l). Followed by the **general procedure E**, compound **14j** as white solid was obtained.  $^1\text{H}$  NMR (600 MHz, DMSO)  $\delta$  9.23 (s, 1H), 8.99 (s, 1H), 8.08 (s, 1H), 7.88 (d,  $J = 8.4$  Hz, 2H), 7.64 (d,  $J = 8.4$  Hz, 2H), 7.54 (d,  $J = 9.0$  Hz, 2H), 6.88 (d,  $J = 9.1$  Hz, 2H), 3.74 – 3.72 (m, 4H), 3.64 (dd,  $J = 10.6, 5.5$  Hz, 8H), 3.04 – 3.01 (m, 4H), 2.51 (s, 3H).  $^{13}\text{C}$  NMR (151 MHz, DMSO)  $\delta$  196.82, 160.51, 158.18, 157.93, 154.91, 146.60, 145.74, 133.25, 130.78, 129.69, 120.70, 118.66, 116.01, 66.63, 49.70, 47.25, 43.95, 26.79. m.p.: 233.7 – 236.8 °C. HPLC purity: 99.16%, retention time = 23.968 min. LC-MS (ESI positive mode)  $m/z$  536.09 ( $[\text{M}+\text{H}]^+$ ).

4.1.9.13. *N*-(4-(2-(4-(2-((4-morpholinophenyl)amino)-5-(trifluoromethyl)pyrimidin-4-yl)piperazine-1-carboxamide) (14m). Followed by the **general procedure E**, compound **14j** as white solid was obtained.  $^1\text{H}$  NMR (600 MHz, DMSO)  $\delta$  9.62 (s, 1H), 8.97 (s, 1H), 8.39 (s, 1H), 7.87 (d,  $J = 8.4$  Hz, 2H), 7.64 (d,  $J = 8.4$  Hz, 2H), 7.54 (d,  $J = 9.0$  Hz, 2H), 6.91 (d,  $J = 9.0$  Hz, 2H), 3.76 – 3.72 (m, 4H), 3.62 (d,  $J = 3.7$  Hz, 8H), 3.08 – 3.03 (m, 4H), 2.51 (s, 3H).  $^{13}\text{C}$  NMR (151 MHz, DMSO)  $\delta$  196.83, 154.83, 147.20, 145.71, 132.26, 130.79, 129.68, 118.65, 115.85, 66.61, 65.38, 49.50, 47.88, 43.81, 26.80, 15.63. m.p.: 213.4 – 215.6 °C. HPLC purity: 99.18%, retention time = 24.832 min. LC-MS (ESI positive mode)  $m/z$  570.01 ( $[\text{M}+\text{H}]^+$ ).

4.1.9.14. *N*-(4-(2-(4-(2-((4-morpholinophenyl)amino)-5-nitropyrimidin-4-yl)piperazine-1-carboxamide) (14n). Followed by the **general procedure E**, compound **14j** as white solid was obtained.  $^1\text{H}$  NMR (600 MHz, DMSO)  $\delta$  10.17 (s, 1H), 8.97 (s, 2H), 8.89 (s, 1H), 7.87 (d,  $J = 7.8$  Hz, 2H), 7.63 (d,  $J = 8.4$  Hz, 2H), 7.58 (s, 1H), 6.94 (d,  $J = 6.0$  Hz, 2H), 3.74 (s, 4H), 3.66 (s, 4H), 3.58 (s, 4H), 3.07 (s, 4H), 2.51 (s, 3H).  $^{13}\text{C}$  NMR (151 MHz, DMSO)  $\delta$  196.82, 154.79, 147.75, 145.69, 131.42, 130.79, 129.68, 121.69, 118.66, 115.71, 66.57, 49.25, 47.81, 43.52, 26.78. m.p.: 253.2 – 257.3 °C. HPLC purity: 96.01%, retention time = 22.877 min. LC-MS (ESI positive mode)  $m/z$  547.1 ( $[\text{M}+\text{H}]^+$ ).

4.1.9.15. *N*-(4-(2-(4-(2-((4-morpholinophenyl)amino)pyrimidin-4-yl)piperazine-1-carboxamide) (14o). To a mixture of **14n** (0.3 g, 0.78 mmol) and Pd-C (0.1 g, 10% m/m) in 5 mL ethanol, then hydrogenated at room temperature for 12 h. After filtration, the filtrate was concentrated. The crude product was further purified by flash column chromatography using DCM/MeOH (30:1) as eluent to afford **14o** as a pale yellow solid.  $^1\text{H}$  NMR (600 MHz, DMSO)  $\delta$  9.02 (s, 1H), 8.52 (s, 1H), 7.88 (d,  $J = 8.4$  Hz, 2H), 7.73 (s, 1H), 7.65 (d,  $J = 8.4$  Hz, 2H), 7.57 (d,  $J = 9.0$  Hz, 2H), 6.84 (d,  $J = 9.0$  Hz, 2H), 4.17 (s, 2H), 3.74 – 3.71 (m, 4H), 3.67 – 3.63 (m, 4H), 3.43 – 3.39 (m, 4H), 3.00 – 2.97 (m, 4H), 2.51 (s, 3H).  $^{13}\text{C}$  NMR (151 MHz, DMSO)  $\delta$  196.83, 155.81, 155.00, 153.73, 145.85, 145.26, 144.13, 135.32, 130.71, 129.67, 124.49, 118.91, 118.66, 116.38, 66.70, 50.14, 46.53, 44.11, 26.79. m.p.: 199.6 – 201.4 °C. HPLC purity: 96.05%, retention time = 17.100 min. LC-MS

(ESI positive mode)  $m/z$  517.07 ( $[M+H]^+$ ).

**4.1.9.16.** 1-(4-(5-methyl-2-((4-morpholinophenyl)amino)pyrimidin-4-yl)piperazin-1-yl)ethan-1-one (**15a**). Followed by the **general procedure F**, compound **15a** as pale yellow solid was obtained.  $^1H$  NMR (600 MHz, DMSO)  $\delta$  8.86 (s, 1H), 7.89 (s, 1H), 7.57 (d,  $J = 9.0$  Hz, 2H), 6.86 (d,  $J = 9.0$  Hz, 2H), 3.73–3.71 (m, 4H), 3.56 (dd,  $J = 10.5, 7.4$  Hz, 4H), 3.42–3.40 (m, 2H), 3.36–3.34 (m, 2H), 3.01–2.99 (m, 4H), 2.10 (s, 3H), 2.04 (s, 3H).  $^{13}C$  NMR (151 MHz, DMSO)  $\delta$  168.92, 164.93, 159.21, 158.70, 145.93, 134.30, 119.93, 116.18, 107.84, 66.67, 49.92, 47.69, 47.38, 45.95, 41.18, 21.73, 16.59. m.p.: 196.3–198.1 °C. HPLC purity: 99.52%, retention time = 12.981 min. LC-MS (ESI positive mode)  $m/z$  397.10 ( $[M+H]^+$ ).

**4.1.9.17.** 5-methyl-4-(4-(methylsulfonyl)piperazin-1-yl)-N-(4-morpholinophenyl)pyrimidin-2-amine (**15b**). Followed by the **general procedure F**, compound **15b** as pale yellow solid was obtained.  $^1H$  NMR (600 MHz, DMSO)  $\delta$  9.33 (s, 1H), 7.85 (s, 1H), 7.39 (d,  $J = 8.4$  Hz, 2H), 6.98 (d,  $J = 9.6$  Hz, 2H), 3.85–3.79 (m, 4H), 3.75–3.73 (m, 5H), 3.11–3.08 (m, 9H), 2.93 (s, 3H), 2.20 (s, 3H).  $^{13}C$  NMR (151 MHz, DMSO)  $\delta$  163.89, 159.10, 158.87, 122.85, 116.05, 107.27, 66.54, 49.23, 46.91, 46.13, 45.65, 34.75, 17.75. m.p.: 256.5–260.6 °C. HPLC purity: 95.31%, retention time = 13.641 min. LC-MS (ESI positive mode)  $m/z$  433.02 ( $[M+H]^+$ ).

**4.1.9.18.** 1-(4-(5-methyl-2-((4-morpholinophenyl)amino)pyrimidin-4-yl)piperazin-1-yl)propan-1-one (**15c**). Followed by the **general procedure F**, compound **15c** as pale yellow solid was obtained.  $^1H$  NMR (600 MHz, DMSO)  $\delta$  8.87 (s, 1H), 7.88 (s, 1H), 7.57 (d,  $J = 8.4$  Hz, 2H), 6.86 (d,  $J = 7.8$  Hz, 2H), 3.72 (s, 4H), 3.57 (d,  $J = 13.2$  Hz, 4H), 3.38 (d,  $J = 28.5$  Hz, 4H), 3.00 (s, 4H), 2.36 (d,  $J = 7.3$  Hz, 2H), 2.10 (s, 3H), 1.01 (t,  $J = 7.2$  Hz, 3H).  $^{13}C$  NMR (151 MHz, DMSO)  $\delta$  172.00, 164.91, 158.98, 158.59, 145.97, 134.22, 119.98, 116.17, 107.83, 66.66, 49.91, 47.70, 47.42, 45.02, 41.35, 26.00, 16.61, 9.81. m.p.: 173.7–176.1 °C. HPLC purity: 97.67%, retention time = 14.566 min. LC-MS (ESI positive mode)  $m/z$  411.03 ( $[M+H]^+$ ).

**4.1.9.19.** N,N-dimethyl-4-(5-methyl-2-((4-morpholinophenyl)amino)pyrimidin-4-yl)piperazine-1-carboxamide (**15d**). Followed by the **general procedure F**, compound **15d** as pale yellow solid was obtained.  $^1H$  NMR (600 MHz, DMSO)  $\delta$  8.83 (s, 1H), 7.88 (s, 1H), 7.58 (d,  $J = 9.0$  Hz, 2H), 6.86 (d,  $J = 9.0$  Hz, 2H), 3.74–3.71 (m, 4H), 3.39–3.36 (m, 4H), 3.24 (m, 4H), 3.02–2.99 (m, 4H), 2.77 (s, 6H), 2.09 (s, 3H).  $^{13}C$  NMR (151 MHz, DMSO)  $\delta$  165.06, 164.17, 159.15, 158.71, 145.91, 134.35, 119.87, 116.20, 107.88, 66.67, 49.94, 47.41, 46.75, 38.53, 16.64. m.p.: 195.3–198.6 °C. HPLC purity: 97.87%, retention time = 15.111 min. LC-MS (ESI positive mode)  $m/z$  426.15 ( $[M+H]^+$ ).

**4.1.9.20.** 1-(4-(5-methyl-2-((4-morpholinophenyl)amino)pyrimidin-4-yl)piperazin-1-yl)pentane-1,4-dione (**15e**). Followed by the **general procedure F**, compound **15e** as white solid was obtained.  $^1H$  NMR (600 MHz, DMSO)  $\delta$  9.82 (s, 1H), 7.69 (s, 1H), 7.31 (d,  $J = 8.4$  Hz, 2H), 7.00 (d,  $J = 9.0$  Hz, 2H), 3.84 (d,  $J = 4.8$  Hz, 2H), 3.79–3.76 (m, 2H), 3.76–3.73 (m, 5H), 3.66–3.64 (m, 2H), 3.60–3.58 (m, 2H), 3.13–3.10 (m, 4H), 2.66 (d,  $J = 6.0$  Hz, 2H), 2.55 (t,  $J = 6.3$  Hz, 2H), 2.23 (s, 3H), 2.12 (s, 4H).  $^{13}C$  NMR (151 MHz, DMSO)  $\delta$  207.91, 170.59, 163.64, 151.61, 129.34, 121.21, 116.01, 107.34, 66.53, 49.01, 46.99, 44.43, 41.22, 37.91, 30.32, 27.06, 17.97. m.p.: 172.5–175.6 °C. HPLC purity: 98.59%, retention time = 13.837 min. LC-MS (ESI positive mode)  $m/z$  453.18 ( $[M+H]^+$ ).

**4.1.9.21.** cyclopropyl(4-(5-methyl-2-((4-morpholinophenyl)amino)pyrimidin-4-yl)piperazin-1-yl)methanone (**15f**). Followed by the **general procedure F**, compound **15f** as white solid was obtained.  $^1H$  NMR (600 MHz, DMSO)  $\delta$  8.99 (s, 1H), 7.88 (s, 1H), 7.56 (d,  $J = 7.2$  Hz, 2H), 6.87

(s, 2H), 3.81 (s, 2H), 3.74–3.70 (m, 4H), 3.60 (s, 2H), 3.49 (s, 2H), 3.41 (s, 2H), 3.01 (s, 4H), 2.12 (s, 3H), 2.00 (dt,  $J = 12.3, 3.9$  Hz, 1H), 0.77 (dd,  $J = 4.3, 2.3$  Hz, 2H), 0.73 (dt,  $J = 11.2, 4.3$  Hz, 2H).  $^{13}C$  NMR (151 MHz, DMSO)  $\delta$  171.74, 164.76, 120.31, 116.16, 107.80, 66.64, 49.82, 47.79, 47.38, 45.13, 41.88, 31.15, 16.75, 12.87, 10.82, 8.14, 7.55. m.p.: 172.8–176.4 °C. HPLC purity: 99.16%, retention time = 15.319 min. LC-MS (ESI positive mode)  $m/z$  423.13 ( $[M+H]^+$ ).

**4.1.9.22.** 4-(4-(cyclopropylsulfonyl)piperazin-1-yl)-5-methyl-N-(4-morpholinophenyl)pyrimidin-2-amine (**15g**). Followed by the **general procedure F**, compound **15g** as pale yellow solid was obtained.  $^1H$  NMR (600 MHz, DMSO)  $\delta$  8.90 (s, 1H), 7.91 (s, 1H), 7.58 (d,  $J = 9.0$  Hz, 2H), 6.87 (d,  $J = 9.0$  Hz, 2H), 3.74–3.71 (m, 4H), 3.49–3.44 (m, 4H), 3.33–3.31 (m, 4H), 3.02–2.98 (m, 4H), 2.65–2.60 (m, 1H), 2.09 (s, 3H), 1.01–0.98 (m, 2H), 0.96–0.93 (m, 2H).  $^{13}C$  NMR (151 MHz, DMSO)  $\delta$  164.85, 159.33, 158.72, 145.99, 134.21, 120.00, 116.17, 108.05, 66.66, 49.91, 47.29, 46.16, 25.14, 16.46, 4.36. m.p.: 196.4–199.7 °C. HPLC purity: 97.52%, retention time = 15.253 min. LC-MS (ESI positive mode)  $m/z$  459.04 ( $[M+H]^+$ ).

**4.1.9.23.** N-(4-acetylphenyl)-4-(5-methyl-2-((4-morpholinophenyl)amino)pyrimidin-4-yl)piperazine-1-sulfonamide (**15h**). Followed by the **general procedure F**, compound **15h** as pale yellow solid was obtained.  $^1H$  NMR (600 MHz, DMSO)  $\delta$  10.57 (s, 1H), 8.86 (s, 1H), 7.91 (d,  $J = 9.0$  Hz, 2H), 7.88 (s, 1H), 7.53 (d,  $J = 8.4$  Hz, 2H), 7.30 (d,  $J = 9.0$  Hz, 2H), 6.85 (d,  $J = 9.0$  Hz, 2H), 3.75–3.71 (m, 4H), 3.39–3.34 (m, 4H), 3.31–3.26 (m, 4H), 3.01 (s, 4H), 2.49 (s, 3H), 2.04 (s, 3H).  $^{13}C$  NMR (151 MHz, DMSO)  $\delta$  196.89, 164.79, 159.29, 158.63, 145.99, 143.47, 134.13, 131.88, 130.25, 119.96, 117.95, 116.16, 66.66, 49.90, 46.99, 46.08, 26.86, 16.34. m.p.: 230.1–237.1 °C. HPLC purity: 96.70%, retention time = 17.654 min. LC-MS (ESI positive mode)  $m/z$  552.15 ( $[M+H]^+$ ).

**4.1.9.24.** N-(4-acetylphenyl)-1-(5-methyl-2-((4-morpholinophenyl)amino)pyrimidin-4-yl)piperidine-4-carboxamide (**16a**). To a solution of **7j** (0.2 g, 0.5 mmol) and DIPEA (0.09 g, 0.75 mmol) in 10 mL 1,4-dioxane, HATU (0.28 g, 0.75 mmol) and 1-(4-aminophenyl)ethan-1-one (0.08 g, 0.6 mmol) were added and the mixture was then stirred at room temperature for 8 h. The resulting mixture was poured into stirring water (10 mL), and then the blue gray solid was filtered and dried under reduced pressure. Using DCM/MeOH (20:1) as eluent to further purify the crude product by flash column chromatography, **16a** as pale yellow solid was obtained.  $^1H$  NMR (600 MHz, DMSO)  $\delta$  10.52 (s, 1H), 10.20 (s, 1H), 7.92 (d,  $J = 8.4$  Hz, 2H), 7.77 (t,  $J = 6.8$  Hz, 3H), 7.36 (d,  $J = 8.4$  Hz, 2H), 7.00 (d,  $J = 7.8$  Hz, 2H), 4.46 (d,  $J = 13.2$  Hz, 2H), 3.75–3.72 (m, 4H), 3.24 (t,  $J = 12.0$  Hz, 2H), 3.13–3.08 (m, 4H), 2.84 (td,  $J = 11.1, 5.5$  Hz, 1H), 2.52 (s, 3H), 2.22 (s, 3H), 1.99 (d,  $J = 10.6$  Hz, 2H), 1.74 (dd,  $J = 22.2, 10.5$  Hz, 2H).  $^{13}C$  NMR (151 MHz, DMSO)  $\delta$  196.95, 173.75, 163.21, 144.10, 132.07, 129.89, 118.85, 116.03, 107.00, 66.47, 62.46, 49.11, 46.99, 42.50, 28.86, 26.88, 25.96, 18.28. m.p.: 284.5–288.1 °C. HPLC purity: 96.03%, retention time = 18.252 min. LC-MS (ESI positive mode)  $m/z$  515.15 ( $[M+H]^+$ ).

**4.1.9.25.** N-(4-cyanophenyl)-1-(5-methyl-2-((4-morpholinophenyl)amino)pyrimidin-4-yl)piperidine-4-carboxamide (**16b**). Followed by the synthesis procedure for **16a**, **16b** as pale yellow solid was obtained.  $^1H$  NMR (600 MHz, DMSO)  $\delta$  10.46 (s, 1H), 8.81 (s, 1H), 7.86 (s, 1H), 7.82 (d,  $J = 8.4$  Hz, 2H), 7.76 (d,  $J = 9.0$  Hz, 2H), 7.60 (d,  $J = 9.0$  Hz, 2H), 6.85 (d,  $J = 9.0$  Hz, 2H), 4.01 (d,  $J = 13.2$  Hz, 2H), 3.73–3.71 (m, 4H), 3.01–2.99 (m, 4H), 2.91 (t,  $J = 11.9$  Hz, 2H), 2.67 (tt,  $J = 11.5, 3.7$  Hz, 1H), 2.10 (s, 3H), 1.91 (d,  $J = 10.8$  Hz, 2H), 1.75 (td,  $J = 12.1, 9.1$  Hz, 2H).  $^{13}C$  NMR (151 MHz, DMSO)  $\delta$  174.54, 165.19, 159.01, 158.73, 145.86, 144.03, 134.46, 133.70, 119.83, 119.58, 116.16, 107.83, 105.21, 66.67, 49.94, 47.24, 43.50, 28.60, 16.69. m.p.: 222.8–224.4 °C. HPLC purity: 99.12%, retention time = 18.654 min. LC-MS (ESI positive mode)  $m/z$  498.11 ( $[M+H]^+$ ).

4.1.9.26. 1-(4-((5-methyl-2-((4-morpholinophenyl)amino)pyrimidin-4-yl)amino)piperidin-1-yl)ethan-1-one (**16c**). Followed by the **general procedure B**, compound **16c** as white solid was obtained.  $^1\text{H}$  NMR (600 MHz, DMSO- $d_6$ )  $\delta$  8.60 (s, 1H), 7.62 (s, 1H), 7.60 (d,  $J = 8.6$  Hz, 2H), 6.84 (d,  $J = 8.6$  Hz, 2H), 6.25 (d,  $J = 7.2$  Hz, 1H), 4.43 (m, 1H), 4.17 (m, 1H), 3.88 (m, 1H), 3.72 (m, 4H), 3.13 (m, 1H), 3.00 (m, 4H), 2.64 (m, 1H), 2.03 (s, 3H), 1.97 (m, 2H), 1.89 (s, 3H), 1.48 (m, 1H), 1.42 – 1.36 (m, 1H).  $^{13}\text{C}$  NMR (151 MHz, DMSO- $d_6$ )  $\delta$  168.38, 160.65, 158.93, 154.33, 145.55, 134.80, 119.53, 116.12, 104.19, 66.60, 49.95, 48.05, 45.56, 40.77, 32.36, 31.55, 21.70, 13.58. m.p.: 286.0 – 291.4 °C. HPLC purity: 99.15%, retention time = 14.417 min. LC-MS (ESI positive mode)  $m/z$  411.15 ( $[\text{M}+\text{H}]^+$ ).

4.1.9.27. *N*-(4-acetylphenyl)-4-((5-methyl-2-((4-morpholinophenyl)amino)pyrimidin-4-yl)amino)piperidine-1-carboxamide (**16d**). Followed by the **general procedure B**, compound **16c** as pale yellow solid was obtained.  $^1\text{H}$  NMR (600 MHz, DMSO- $d_6$ )  $\delta$  8.95 (s, 1H), 8.61 (s, 1H), 7.87 (d,  $J = 7.9$  Hz, 2H), 7.63 (m, 5H), 6.85 (d,  $J = 7.8$  Hz, 2H), 6.29 (d,  $J = 5.4$  Hz, 1H), 4.30 – 4.07 (m, 3H), 3.72 (d,  $J = 2.2$  Hz, 4H), 3.00 (d,  $J = 2.2$  Hz, 4H), 2.95 (t,  $J = 12.9$  Hz, 2H), 2.50 (s, 3H), 1.96 (d,  $J = 11.6$  Hz, 2H), 1.90 (s, 3H), 1.54 (q,  $J = 12.0$  Hz, 2H).  $^{13}\text{C}$  NMR (151 MHz, DMSO- $d_6$ )  $\delta$  196.73, 160.67, 158.94, 154.69, 154.35, 145.92, 145.56, 134.83, 130.53, 129.58, 119.52, 118.51, 116.14, 66.59, 56.40, 49.96, 48.10, 43.93, 31.84, 26.71, 18.94, 13.60. m.p.: 245.4 – 247.5 °C. HPLC purity: 98.30%, retention time = 17.964 min. LC-MS (ESI positive mode)  $m/z$  530.20 ( $[\text{M}+\text{H}]^+$ ).

4.1.9.28. *N*-(4-acetylphenyl)-3-((5-methyl-2-((4-morpholinophenyl)amino)pyrimidin-4-yl)amino)pyrrolidine-1-carboxamide (**16e**). Followed by the **general procedure B**, compound **16e** as white solid was obtained.  $^1\text{H}$  NMR (600 MHz, DMSO)  $\delta$  8.69 (s, 1H), 8.58 (s, 1H), 7.86 (d,  $J = 9.0$  Hz, 2H), 7.71 (d,  $J = 9.0$  Hz, 2H), 7.66 (s, 1H), 7.58 (d,  $J = 9.0$  Hz, 2H), 6.82 (d,  $J = 9.0$  Hz, 2H), 6.66 (d,  $J = 5.4$  Hz, 1H), 3.91 – 3.87 (m, 1H), 3.69 – 3.66 (m, 4H), 3.64 – 3.61 (m, 1H), 3.51 – 3.47 (m, 1H), 3.37 (dd,  $J = 6.5, 3.7$  Hz, 1H), 2.95 – 2.92 (m, 4H), 2.50 (s, 3H), 2.22 (d,  $J = 6.1$  Hz, 1H), 2.13 – 2.05 (m, 2H), 1.94 (s, 3H).  $^{13}\text{C}$  NMR (151 MHz, DMSO)  $\delta$  196.80, 161.31, 153.88, 145.86, 130.55, 129.66, 120.02, 118.40, 116.15, 104.72, 66.63, 51.47, 49.89, 44.74, 26.77, 13.71. m.p.: 214.3 – 215.4 °C. HPLC purity: 99.85%, retention time = 16.716 min. LC-MS (ESI positive mode)  $m/z$  516.18 ( $[\text{M}+\text{H}]^+$ ).

4.1.9.29. *N*-(4-acetylphenyl)-3-((5-methyl-2-((4-morpholinophenyl)amino)pyrimidin-4-yl)amino)azetidine-1-carboxamide (**16f**). Followed by the **general procedure B**, compound **16f** as pale yellow solid was obtained.  $^1\text{H}$  NMR (600 MHz, DMSO)  $\delta$  9.69 (s, 1H), 9.47 (s, 1H), 7.87 (s, 1H), 7.85 (d,  $J = 8.4$  Hz, 2H), 7.54 (d,  $J = 8.4$  Hz, 2H), 7.33 (d,  $J = 9.0$  Hz, 2H), 7.16 (s, 1H), 6.93 (d,  $J = 9.0$  Hz, 2H), 4.58 – 4.51 (m, 2H), 4.32 (t,  $J = 9.0$  Hz, 1H), 3.75 – 3.72 (m, 4H), 3.54 – 3.50 (m, 1H), 3.41 (d,  $J = 14.0$  Hz, 1H), 3.10 – 3.07 (m, 4H), 2.49 (s, 3H), 2.01 (s, 3H).  $^{13}\text{C}$  NMR (151 MHz, DMSO)  $\delta$  196.66, 157.75, 155.94, 149.48, 149.01, 145.45, 130.36, 130.07, 129.13, 125.15, 117.05, 115.45, 66.53, 50.40, 49.01, 42.71, 26.74, 12.44. m.p.: 147.9 – 151.6 °C. HPLC purity: 99.46%, retention time = 15.628 min. LC-MS (ESI positive mode)  $m/z$  502.10 ( $[\text{M}+\text{H}]^+$ ).

4.1.9.30. 1-(4-acetylphenyl)-3-(1-(5-methyl-2-((4-morpholinophenyl)amino)pyrimidin-4-yl)pyrrolidin-3-yl)urea (**16g**). Followed by the **general procedure B**, compound **16g** as white solid was obtained.  $^1\text{H}$  NMR (600 MHz, DMSO)  $\delta$  9.51 (s, 1H), 9.20 (s, 1H), 7.85 (d,  $J = 8.4$  Hz, 2H), 7.66 (s, 1H), 7.52 (d,  $J = 9.0$  Hz, 2H), 7.47 (d,  $J = 8.4$  Hz, 2H), 7.08 (d,  $J = 6.6$  Hz, 1H), 6.91 (d,  $J = 9.0$  Hz, 2H), 4.29 (d,  $J = 4.8$  Hz, 1H), 3.98 (dd,  $J = 10.8, 5.4$  Hz, 1H), 3.92 – 3.83 (m, 2H), 3.75 – 3.70 (m, 4H), 3.67 (dd,  $J = 11.4, 3.1$  Hz, 1H), 3.04 (s, 4H), 2.49 (s, 3H), 2.26 (s, 3H), 2.15 (t,  $J = 12.7$  Hz, 1H), 1.91 (dd,  $J = 11.2, 5.7$  Hz, 1H).  $^{13}\text{C}$  NMR (151 MHz, DMSO)  $\delta$  196.63, 161.26, 155.04, 145.43, 130.31, 130.09, 121.75,

116.96, 116.02, 66.59, 55.24, 53.86, 49.41, 49.12, 47.87, 31.03, 26.73, 17.29. m.p.: 157.4 – 160.1 °C. HPLC purity: 97.69%, retention time = 17.666 min. LC-MS (ESI positive mode)  $m/z$  516.18 ( $[\text{M}+\text{H}]^+$ ).

4.1.9.31. 1-(4-acetylphenyl)-3-(1-(5-methyl-2-((4-morpholinophenyl)amino)pyrimidin-4-yl)azetidin-3-yl)urea (**16h**). Followed by the **general procedure B**, compound **16h** as white solid was obtained.  $^1\text{H}$  NMR (600 MHz, DMSO)  $\delta$  10.14 (s, 1H), 9.54 (s, 1H), 7.86 (d,  $J = 8.4$  Hz, 2H), 7.62 (s, 1H), 7.57 (t,  $J = 6.6$  Hz, 3H), 7.42 (d,  $J = 8.4$  Hz, 2H), 6.96 (d,  $J = 9.0$  Hz, 2H), 4.82 – 4.54 (m, 2H), 4.44 – 4.20 (m, 2H), 3.74 – 3.72 (m, 4H), 3.09 – 3.06 (m, 4H), 2.49 (s, 3H), 2.10 (s, 3H).  $^{13}\text{C}$  NMR (151 MHz, DMSO)  $\delta$  196.69, 161.58, 154.88, 145.41, 130.50, 130.04, 117.29, 115.94, 106.05, 66.55, 49.13, 40.78, 26.74, 14.26. m.p.: 178.1 – 182.1 °C. HPLC purity: 98.17%, retention time = 17.455 min. LC-MS (ESI positive mode)  $m/z$  502.10 ( $[\text{M}+\text{H}]^+$ ).

## 4.2. Biological section

### 4.2.1. JAK2 and FLT3 kinases assays

The *in vitro* kinase assays of designed compounds against JAK2 and FLT3 were performed by Shanghai ChemPartner Co. Ltd. (China). Briefly, the compounds, enzyme (JAK2 and FLT3 both from Carna), and ATP (25 mM, Sigma) were diluted in kinase buffer to the indicated concentrations. 5  $\mu\text{L}$  of compound in kinase buffer and the prepared enzyme solution were added to each well and incubated at room temperature for 10 min. Then, 10  $\mu\text{L}$  of prepared FAM-labeled peptide and ATP solution was added. After the incubation at 28 °C for 60 min, 25  $\mu\text{L}$  of stop buffer was added. The data was collected on Caliper program, and  $\text{IC}_{50}$  values were calculated from the inhibition curves.

### 4.2.2. Cell growth inhibition assay

Cell proliferation was determined by CCK-8 assay. Cell lines (HEL 3000 cells/well, Molm-13 5000 cells/well, K562 3000 cells/well and PC-3 5000 cells/well) were seeded in 96-well plates with RPMI1640 (Gibco) containing 10% FBS and 1% penicillin-streptomycin (Gibco). The cells were then treated with increasing concentrations of compounds. After incubating for 48 h, 20  $\mu\text{L}$  of CCK-8 (Solarbio) was added to each well and incubated for an additional 4 h. Then, the plates were swayed for 5 min and were read at 450 nm by using a microplate reader (Synergy HT, BioTek). All the experiments were repeated at least three times. Dose-response curves were obtained by Prism 5.0 (GraphPad Software).

### 4.2.3. *In vitro* drug metabolism in rat liver microsomes

The selected compounds were determined in microsomes for two parallel determinations with or without the NADPH regenerating system. Briefly, the compounds were preincubated with microsomes (rat microsomes, Xenotech, Lot No. 1310030) (0.5 mg/mL) at 1 mM for 10 min at 37 °C in potassium phosphate buffer (100 mM at pH 7.4 with 10 mM  $\text{MgCl}_2$ ). As a positive control, a solution of 7-ethoxycoumarin (1 mM) was used. Then, pre-warmed cofactors (1 mmol NADPH) were added to initiated the reactions. Cold acetonitrile was added to precipitate the protein after incubation for different times (0, 5, 10, 20, 30, and 60 min) at 37 °C, and the samples were subsequently centrifuged. At last, the supernatants were analyzed by LC-MS/MS.

### 4.2.4. Flow cytometry assay

The Flow cytometry Assays were done by Takara Biotech (Shenyang, China). Briefly, Molm-13 cells ( $3 \times 10^5$  cells/mL) were seeded in 6-well plates and incubated for 12 h, then different concentrations of tested compound **14l** were added to each well and incubated for a further 48 h. Followed by a standard propidium iodide (PI) staining procedure, the cell cycle distribution samples were obtained. Followed by the operating instructions of the kit, cells were treated by Annexin-V and PI double staining, then the cell apoptosis samples were obtained. These samples

were analyzed under 488 nm by a FACScan Cytometer (FACS Calibur, Becton Dickinson, Franklin Lakes, NJ).

#### 4.3. Molecular docking

The 2D structures of molecules were generated by ChemDraw, then converted to 3D structures using Maestro LigPrep, version 2.1.207. The X-ray structure of JAK2 (PDB code 4JI9) was obtained from the Protein Data Bank. The FLT3 homology modelling structure was obtained from a DFG-peptide modification based on PDB code 1RJB, which was a released FLT3 protein structure with the DFG-out conformation. The modification was made to carry out molecular-dynamics modelling (30 ns) with restraints on DFG peptide to induce a DFG-in mode. Here the restrained molecular dynamics were run using TINKER 4.223 with an amber99 force field. Then from the trajectory of FLT3 DFG-in conformations, a conformation with the minimum RMSD compared with PDB structure 1RJB was used as our FLT3 DFG-in conformation[26]. The Grid files were obtained following the standard procedure recommended by Schrödinger. The 3D structures were docked flexibly using Glide in XP mode, and other docking parameters were set to default values. Ten predicted poses were obtained during the docking process, and the Grid-based score was calculated for each pose. The image files were generated by PyMOL (version 1.7).

#### Declaration of Competing Interest

The authors declare that they have no known competing financial interests or personal relationships that could have appeared to influence the work reported in this paper.

#### Acknowledgements

The work was supported by LiaoNing Revitalization Talents Program (Grant No. XLYC1805014 and XLYC1808037).

#### Appendix A. Supplementary data

Supplementary data to this article can be found online at <https://doi.org/10.1016/j.bioorg.2020.104361>.

#### References

- [1] K.M. Bernot, J.S. Nemer, R. Santhanam, S. Liu, N.A. Zorko, S.P. Whitman, K. E. Dickerson, M. Zhang, X. Yang, K.K. McConnell, E.H. Ahmed, M.R. Munoz, R. F. Siebenaler, G.G. Marcucci, B.L. Mundy-Bosse, D.L. Brook, S. Garman, A. M. Dorrance, X. Zhang, J. Zhang, R.J. Lee, W. Blum, M.A. Caligiuri, G. Marcucci, Eradicating acute myeloid leukemia in a MLL(PTD/wt):FLT3(ITD/wt) murine model: a path to novel therapeutic approaches for human disease, *Blood* 122 (2013) 3778–3783.
- [2] S. Piya, S.M. Kornblau, V.R. Ruvolo, H. Mu, P.P. Ruvolo, T. McQueen, R.E. Davis, N. Hail Jr., H. Kantarjian, M. Andreeff, G. Borthakur, Atg7 suppression enhances chemotherapeutic agent sensitivity and overcomes stroma-mediated chemoresistance in acute myeloid leukemia, *Blood* 128 (2016) 1260–1269.
- [3] O. Rosnet, C. Schiff, M.J. Pebusque, S. Marchetto, C. Tonnelle, Y. Toiron, F. Birg, D. Birnbaum, Human FLT3/FLK2 gene: cDNA cloning and expression in hematopoietic cells, *Blood* 82 (1993) 1110–1119.
- [4] H.G. Drexler, Expression of FLT3 receptor and response to FLT3 ligand by leukemic cells, *Leukemia* 10 (1996) 588–599.
- [5] D.L. Stirewalt, J.P. Radich, The role of FLT3 in haematopoietic malignancies, *Nat. Rev. Cancer* 3 (2003) 650–665.
- [6] D. Fabbro, E. Buchdunger, J. Wood, J. Mestan, F. Hofmann, S. Ferrari, H. Mett, T. O'Reilly, T. Meyer, Inhibitors of protein kinases: CGP 41251, a protein kinase inhibitor with potential as an anticancer agent, *Pharmacol. Therapeut.* 82 (1999) 293–301.
- [7] M. Mori, N. Kaneko, Y. Ueno, M. Yamada, R. Tanaka, R. Saito, I. Shimada, K. Mori, S. Kuromitsu, Gilteritinib, a FLT3/AXL inhibitor, shows antileukemic activity in mouse models of FLT3 mutated acute myeloid leukemia, *Invest. New Drugs* 35 (2017) 556–565.
- [8] P.P. Zarrinkar, R.N. Gunawardane, M.D. Cramer, M.F. Gardner, D. Brigham, B. Belli, M.W. Karaman, K.W. Pratz, G. Pallares, Q. Chao, AC220 is a uniquely potent and selective inhibitor of FLT3 for the treatment of acute myeloid leukemia (AML), *Blood* 114 (2009) 2984–2992.
- [9] A.S. Moore, A. Faisal, D. Gonzalez de Castro, V. Bavetsias, C. Sun, B. Atrash, M. Valenti, A. de Haven Brandon, S. Avery, D. Mair, F. Mirabella, J. Swansbury, A. D. Pearson, P. Workman, J. Blagg, F.I. Raynaud, S.A. Eccles, S. Linardopoulos, Selective FLT3 inhibition of FLT3-ITD+ acute myeloid leukaemia resulting in secondary D835Y mutation: a model for emerging clinical resistance patterns, *Leukemia* 26 (2012) 1462–1470.
- [10] C.C. Smith, Q. Wang, C.-S. Chin, S. Salerno, L.E. Damon, M.J. Levis, A.E. Perl, K. J. Travers, S. Wang, J.P. Hunt, Validation of ITD mutations in FLT3 as a therapeutic target in human acute myeloid leukaemia, *Nature* 485 (2012) 260–263.
- [11] T. Yuan, B.W. Qi, Z.L. Jiang, W.J. Dong, L. Zhong, L. Bai, R.S. Tong, J.Y. Yu, J. Y. Shi, Dual FLT3 inhibitors: Against the drug resistance of acute myeloid leukemia in recent decade, *Eur. J. Med. Chem.* 178 (2019) 468–483.
- [12] A.E. Perl, G. Martinelli, J.E. Cortes, A. Neubauer, E. Berman, S. Paolini, P. Montesinos, M.R. Baer, R.A. Larson, C. Ustun, F. Fabbiano, H.P. Erba, A. Di Stasi, R. Stuart, R. Olin, M. Kasner, F. Cicceri, W.C. Chou, N. Podoltsev, C. Recher, H. Yokoyama, N. Hosono, S.S. Yoon, J.H. Lee, T. Pardee, A.T. Fathi, C. Liu, N. Hasabou, X. Liu, E. Bahceci, M.J. Levis, Gilteritinib or Chemotherapy for Relapsed or Refractory FLT3-Mutated AML, *N. Engl. J. Med.* 381 (2019) 1728–1740.
- [13] Z. Li, X. Wang, J. Eksterowicz, M.W. Gribble Jr., G.Q. Alba, M. Ayres, T.J. Carlson, A. Chen, X. Chen, R. Cho, R.V. Connors, M. DeGraffenreid, J.T. Deignan, J. Duquette, P. Fan, B. Fisher, J. Fu, J.N. Huard, J. Kaizerman, K.S. Keegan, C. Li, K. Li, Y. Li, L. Liang, W. Liu, S.E. Lively, M.C. Lo, J. Ma, D.L. McMinn, J.T. Mihalic, K. Modi, R. Ngo, K. Pattabiraman, D.E. Piper, C. Queva, M.L. Ragains, J. Suchomel, S. Thibault, N. Walker, X. Wang, Z. Wang, M. Wanska, P.M. Wehn, M.F. Weidner, A.J. Zhang, X. Zhao, A. Kamb, D. Wickramasinghe, K. Dai, L.R. McGee, J. C. Medina, Discovery of AMG 925, a FLT3 and CDK4 dual kinase inhibitor with preferential affinity for the activated state of FLT3, *J. Med. Chem.* 57 (2014) 3430–3449.
- [14] A.D. William, A.C.H. Lee, S. Blanchard, A. Poulsen, E.L. Teo, H. Nagaraj, E. Tan, D. Z. Chen, M. Williams, E.T. Sun, K.C. Goh, W.C. Ong, S.K. Goh, S. Hart, R. Jayaraman, M.K. Pasha, K. Ethirajulu, J.M. Wood, B.W. Dymock, Discovery of the Macrocyclic 11-(2-Pyrrolidin-1-yl-ethoxy)-14,19-dioxo-5,7,26-triaza-tetracyclo 19.3. 1.1(2,6).1(8,12) heptacos-1(25),2(26),3,5,8,10,12(27),16,21,23-decaene (SB1518), a Potent Janus Kinase 2/Fms-Like Tyrosine Kinase-3 (JAK2/FLT3) Inhibitor for the Treatment of Myelofibrosis and Lymphoma, *J. Med. Chem.*, 54 (2011) 4638–4658.
- [15] A.M. Cook, L. Li, Y. Ho, A. Lin, L. Li, A. Stein, S. Forman, D. Perrotti, R. Jove, R. Bhatia, Role of altered growth factor receptor-mediated JAK2 signaling in growth and maintenance of human acute myeloid leukemia stem cells, *Blood* 123 (2014) 2826–2837.
- [16] M. Dosi, S. Wang, I.R. Lemischka, Mitogenic signalling and substrate specificity of the Flk2/Flt3 receptor tyrosine kinase in fibroblasts and interleukin 3-dependent hematopoietic cells, *Mol. Cell Biol.* 13 (1993) 6572–6585.
- [17] J.B. Zhou, C.L. Bi, J.V. Janakakumara, S.C. Liu, W.J. Chng, K.G. Tay, L.F. Poon, Z. G. Xie, S. Palaniyandi, H. Yu, K.B. Glaser, D.H. Albert, S.K. Davidson, C.S. Chen, Enhanced activation of STAT pathways and overexpression of survivin confer resistance to FLT3 inhibitors and could be therapeutic targets in AML, *Blood* 113 (2009) 4052–4062.
- [18] C.N. Harrison, N. Schaap, A.M. Vannucchi, J.J. Kiladjan, E. Jourdan, R.T. Silver, H.C. Schouten, F. Passamonti, S. Zweegman, M. Talpaz, S. Verstovsek, S. Rose, J. Shen, T. Berry, C. Brownstein, R.A. Mesa, Fedratinib in patients with myelofibrosis previously treated with ruxolitinib: An updated analysis of the JAKART2 study using stringent criteria for ruxolitinib failure, *Am. J. Hematol.* 95 (2020) 594–603.
- [19] Cortellis Drug Discovery Intelligence, in, pp. The Development Status of Pacritinib.
- [20] Y.X. Li, T.Y. Ye, L. Xu, Y.H. Dong, Y. Luo, C. Wang, Y.F. Han, K. Chen, M.Z. Qin, Y. J. Liu, Y.F. Zhao, Discovery of 4-piperazinyl-2-aminopyrimidine derivatives as dual inhibitors of JAK2 and FLT3, *Eur. J. Med. Chem.* 181 (2019) 18.
- [21] P-Loop, in: *Encyclopedia of Genetics, Genomics, Proteomics and Informatics*, Springer Netherlands, Dordrecht, 2008, pp. 1514–1514.
- [22] N.L. Alicea-Velazquez, T.J. Boggan, The use of structural biology in Janus kinase targeted drug discovery, *Curr. Drug Targets* 12 (2011) 546–555.
- [23] S. Martínez-González, A.B. García, M.I. Albarrán, A. Cebriá, A. Amezcua-Alves, F. J. García-Campos, J. Martínez-Gago, J. Martínez-Torrecuadrada, I. Muñoz, C. Blanco-Aparicio, Pyrido [2, 3-b][1, 5] benzoxazepin-5 (6H)-one derivatives as CDK8 inhibitors, *Eur. J. Med. Chem.* 112443 (2020).
- [24] B.B. Hansen, T.H. Jepsen, M. Larsen, R. Sindet, T. Vifian, M.N. Burhardt, J. Larsen, J.G. Seitzberg, M.A. Carnerup, A. Jerre, Fragment-based discovery of pyrazolopyridones as JAK1 inhibitors with excellent subtype selectivity, *J. Med. Chem.* (2020).
- [25] D. Sun, Y. Yang, J. Lyu, W. Zhou, W. Song, Z. Zhao, Z. Chen, Y. Xu, H. Li, Discovery and Rational Design of Pteridin-7(8H)-one-Based Inhibitors Targeting FMS-like Tyrosine Kinase 3 (FLT3) and Its Mutants, *J. Med. Chem.* 59 (2016) 6187–6200.
- [26] Y. Wang, Y. Zhi, Q. Jin, S. Lu, G. Lin, H. Yuan, T. Yang, Z. Wang, C. Yao, J. Ling, Discovery of 4-(7-H-Pyrrolo [2, 3-d] pyrimidin-4-yl) amino-N-(4-(4-methylpiperazin-1-yl) methyl) phenyl)-1-H-pyrazole-3-carboxamide (FN-1501), an FLT3-and CDK-Kinase Inhibitor with Potentially High Efficiency against Acute Myelocytic Leukemia, *J. Med. Chem.* 61 (2018) 1499–1518.